



HAL
open science

Multi-mode solitons in the classical Dicke-Jaynes-Cummings-Gaudin Model.

Olivier Babelon, Benoît Douçot

► **To cite this version:**

Olivier Babelon, Benoît Douçot. Multi-mode solitons in the classical Dicke-Jaynes-Cummings-Gaudin Model.. 2012. hal-00678267

HAL Id: hal-00678267

<https://hal.science/hal-00678267>

Preprint submitted on 12 Mar 2012

HAL is a multi-disciplinary open access archive for the deposit and dissemination of scientific research documents, whether they are published or not. The documents may come from teaching and research institutions in France or abroad, or from public or private research centers.

L'archive ouverte pluridisciplinaire **HAL**, est destinée au dépôt et à la diffusion de documents scientifiques de niveau recherche, publiés ou non, émanant des établissements d'enseignement et de recherche français ou étrangers, des laboratoires publics ou privés.

Multi-mode solitons in the classical Dicke-Jaynes-Cummings-Gaudin Model.

O. Babelon, B. Douçot
Laboratoire de Physique Théorique et Hautes Energies*(LPTHE)
Unité Mixte de Recherche UMR 7589
Université Pierre et Marie Curie-Paris 6 and CNRS;

March 12, 2012

Abstract: We present a detailed analysis of the classical Dicke-Jaynes-Cummings-Gaudin integrable model, which describes a system of n spins coupled to a single harmonic oscillator. We focus on the singularities of the vector-valued moment map whose components are the $n + 1$ mutually commuting conserved Hamiltonians. The level sets of the moment map corresponding to singular values may be viewed as degenerate and often singular Arnold-Liouville torii. A particularly interesting example of singularity corresponds to unstable equilibrium points where the rank of the moment map is zero, or singular lines where the rank is one. The corresponding level sets can be described as a reunion of smooth strata of various dimensions. Using the Lax representation, the associated spectral curve and the separated variables, we show how to construct explicitly these level sets. A main difficulty in this task is to select, among possible complex solutions, the physically admissible family for which all the spin components are real. We obtain explicit solutions to this problem in the rank zero and one cases. Remarkably this corresponds exactly to solutions obtained previously by Yuzbashyan and whose geometrical meaning is therefore revealed. These solutions can be described as multi-mode solitons which can live on strata of arbitrary large dimension. In these solitons, the energy initially stored in some excited spins (or atoms) is transferred at finite times to the oscillator mode (photon) and eventually comes back into the spin subsystem. But their multi-mode character is reflected by a large diversity in their shape, which is controlled by the choice of the initial condition on the stratum.

1 Introduction.

The Dicke model has been used for more than fifty years in atomic physics to describe the interaction of an ensemble of two-level atoms with the quantized electromagnetic field [1]. Recently,

*Tour 13-14, 4ème étage, Boite 126, 4 Place Jussieu, 75252 Paris Cedex 05.

many experimental and theoretical works have considered systems in an optical cavity where matter is coupled to a single eigenmode of the field [2, 3]. These systems offer some unprecedented opportunities to realize quantum bits and to process quantum information. The integrable version of the monomode Dicke model considered in this paper [4, 5] is obtained by making the so called rotating wave approximation in which the non resonant terms (e.g. for which a photon is created while an atom is excited) are discarded. In the case of a single atom, this model has been solved by Jaynes-Cummings [6], and has been used to study the effect of field quantization on Rabi oscillations [7]. In the many atom case, besides the development of cavity QED [2] and circuit QED [3] already mentioned, a surge of interest in the Dicke-Jaynes-Cummings-Gaudin model has been motivated in the context of cold atoms systems, where a sudden change in the interactions between atoms is achieved by sweeping the external magnetic field through a Feshbach resonance [8, 9]. The subsequent dynamics of the atomic system is well described by the DJCG model prepared in the quantum counterpart of a classically unstable equilibrium state.

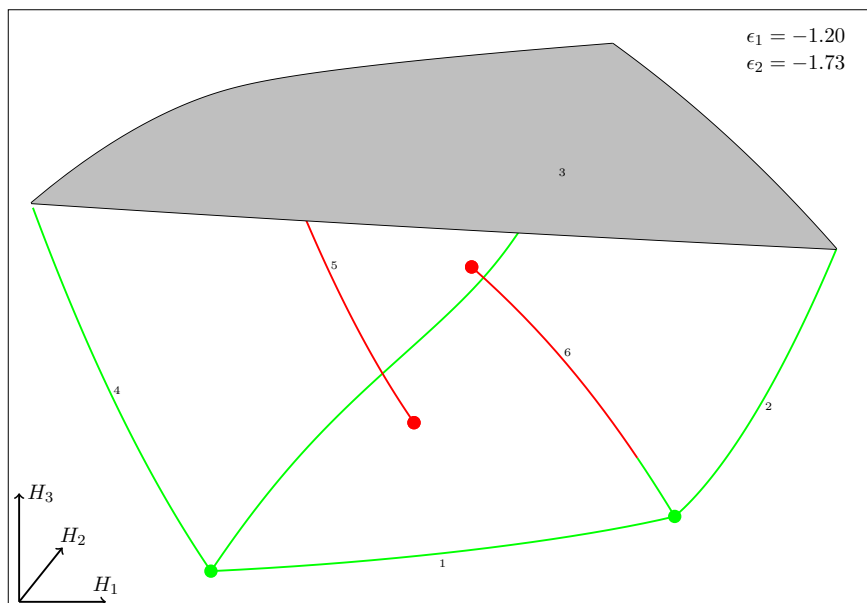


Figure 1: The image of the moment map for the two spins model. The green dots refer to stable (elliptic) equilibrium points. The red dots are unstable (focus-focus) equilibrium points. The preimage of a point on a green line is a Liouville torus degenerated to a circle on which the rank of the moment map is one. The preimage of a point on a red line is a pinched torus times a circle. The parameters (ϵ_1, ϵ_2) are chosen so that we have two elliptic and two focus-focus critical points.

This motivates the study of unstable equilibrium points in classical and quantum integrable models. From the classical viewpoint, an integrable system with n degrees of freedom is characterized by a collection of n mutually commuting functions H_1, H_2, \dots, H_n over the $2n$ -dimensional phase space. Usually, the physical Hamiltonian H is expressed as a function of these conserved quantities. Besides the classical trajectories generated by H , it is of great interest to consider the so-called moment map, which associates to any point p in phase space the n -vector $(H_1(p), H_2(p), \dots, H_n(p))$. The image of the moment map is of great importance. Fig.[1] provides an example of such an image of the moment map for the two spins Dicke-Jaynes-Cummings-Gaudin model. To each point (H_1, H_2, \dots, H_n) in this image corresponds a level set in phase space, that is to say the set of points p such that $(H_1(p) = H_1, H_2(p) = H_2, \dots, H_n(p) = H_n)$. For many systems of physical relevance these level sets are compact (as it is the case here). In the case of a regular value of the moment map, the Arnold-Liouville theorem states that the corresponding level set is an n -dimensional torus. Non regular values of the moment map, (for which the rank of the moment map may be $< n$), are in some sense more interesting, because they correspond to special torii whose dimension may be lower than n or which may contain singular submanifolds. The image of the moment map and its critical values encode all the information on the fibration of phase space in Liouville torii. It is important to realize that the level set of a non-regular value of the moment map is in general a stratified manifold on which the rank of the moment map may jump. The dimension of each stratum is equal to the rank of the differential of the moment map on that stratum.

An extreme case is given by the level set containing an equilibrium point. By definition, the gradient of the moment map vanishes at such point (the rank is zero), which is then an equilibrium point for any Hamiltonian expressed in terms of H_1, H_2, \dots, H_n . For a purely elliptic equilibrium point, the level set is reduced to this point. But for an unstable point, the level set contains the equilibrium point, of course, but also a whole manifold whose description is far from trivial. In the vicinity of the unstable critical point, the stratification can be qualitatively understood by the quadratic normal form [10], deduced from the Taylor expansion of the moment map to second order in the deviations from the critical point. A detailed derivation of these normal forms in the Dicke-Jaynes-Cummings-Gaudin model has been presented in our previous contribution [11]. But the information contained in the normal form is purely local, and it is not sufficient to describe globally the level set containing an unstable critical point. Global characteristics can be accessed by viewing these level sets as collections of trajectories, solutions of the equations of motion. In this paper, we shall present explicit solutions of the physical Hamiltonian equations of motion for an arbitrary initial condition chosen on such a critical level set. They can be described as solitonic pulses in which the energy initially stored in some excited spins (or atoms) is transferred at finite times to the oscillator mode (photon) and eventually comes back into the spin subsystem.

We achieve this by using the well known algebro-geometric solution [13, 15, 14] of the classical Dicke-Jaynes-Cummings-Gaudin model. A key feature of this approach is that the knowledge of the conserved quantities H_1, H_2, \dots, H_{n+1} , (equivalently a point in the image of the moment map) is encoded in a Riemann surface, called the spectral curve. It is of genus $g = n$, where n is the number of spins. The state of the system can be represented by a collection of g points on the spectral

curve. Remarkably, the image of this collection of g points by the Abel map follows a straight line with a constant velocity on the Jacobian torus associated to the spectral curve. This construction linearizes the Hamiltonian flows of the model.

It is well known that critical values of the moment map correspond to degenerate spectral curves [16, 13], and this seems to be the most efficient way to locate the critical values of the moment map. This strategy has been used extensively in our previous discussion of the moment map in the classical Dicke-Jaynes-Cummings-Gaudin model [11]. We believe that the separated variables, which we will use in their Sklyanin presentation [15], are a powerful tool to uncover the stratification of a critical level set. In this paper, we show that each stratum of dimension $n + 1 - n_0$ on such level set is obtained by freezing n_0 separated variables on some zeros of the polynomial which defines the spectral curve.

We will also pay a special attention to the problem of finding the physical slice on each stratum. This is not a straightforward question, because the algebro-geometric method is naturally suited to solve equations of motion in the complexified phase-space. But only solutions for which all spin components and the two oscillator coordinates are real are admissible physically. The determination of the physical slice for a generic regular value of the moment map remains an open problem. But on the critical level sets of the moment map, corresponding to a spectral curve of genus zero, the problem greatly simplifies. This corresponds to level sets of the moment map containing critical points of rank zero or one for which we are able to derive an explicit solution for an arbitrary number of spins. Remarkably these solutions were already constructed by Yuzbashyan [12], and they find here their place in a broader picture aiming at organizing all particular solutions of the Dicke-Jaynes-Cummings-Gaudin model.

This paper is organized as follows. Section 2 presents the classical Dicke-Jaynes-Cummings-Gaudin model of n spins coupled to a single harmonic oscillator, together with the main features of the algebro-geometric solution. In particular, we emphasize that the separated variables capture in a very natural way the stratification of a critical level set, each stratum being characterized by a subset of frozen variables on some double roots of the spectral polynomial. These notions are then illustrated in section 3 on the example of the system with only one spin. In this case, the reality conditions can be worked out explicitly, both on the critical level sets associated to unstable equilibrium points and for generic values of the moment map. Section 4 gives the complete determination of the real slice for the level set of an equilibrium point, and for arbitrary values of n . This corresponds to the case where all the roots of the spectral polynomial are doubly degenerate. We recover here the *normal solitons* first constructed by Yuzbashyan [12]. Section 5 addresses the same question, in the slightly more common situation where the spectral polynomial has n doubly degenerate roots and two simple roots. In this case, we are describing a level set whose smallest stratum has dimension 1. The corresponding values of the moment map lie on curves in its n -dimensional target space. We benefit in this case from the fact that the spectral curve remains rational. We get therefore a general formula for the *anomalous solitons* in Yuzbashyan's terminology. Section 6 illustrates this general theory for the system with two spins, and section 7 for the system with three spins. We present explicit examples of solitonic pulses corresponding to solutions

living in strata of dimensions 2, 3, and 4. The presence of several directions of instability away from the corresponding equilibrium points is reflected by the non-monotonous time dependence seen in these pulses, which contrasts with the simple shape observed for the model with a single spin. Our conclusions are stated in section 8. Finally, an Appendix provides a brief summary of the construction [11] of quadratic normal forms of the moment map in the vicinity of equilibrium points.

2 The classical Dicke-Jaynes-Cummings-Gaudin model.

2.1 Integrability

This model, describes a collection of n spins coupled to a single harmonic oscillator. It derives from the Hamiltonian:

$$H = \sum_{j=1}^n (2\epsilon_j + \omega) s_j^z + \omega \bar{b} b + \sum_{j=1}^n (\bar{b} s_j^- + b s_j^+) \quad (1)$$

The \vec{s}_j are spin variables, and b, \bar{b} is a harmonic oscillator. The Poisson brackets read:

$$\{s_j^a, s_j^b\} = -\epsilon_{abc} s_j^c, \quad \{b, \bar{b}\} = i \quad (2)$$

The \vec{s}_j brackets are degenerate. We fix the value of the Casimir functions

$$\vec{s}_j \cdot \vec{s}_j = s^2$$

Phase space has dimension $2(n+1)$. In the Hamiltonian we have used $s_j^\pm = s_j^1 \pm i s_j^2$ which have Poisson brackets $\{s_j^z, s_j^\pm\} = \pm i s_j^\pm$, $\{s_j^+, s_j^-\} = 2i s_j^z$. The equations of motion read:

$$\dot{b} = -i\omega b - i \sum_{j=1}^n s_j^- \quad (3)$$

$$\dot{s}_j^z = i(\bar{b} s_j^- - b s_j^+) \quad (4)$$

$$\dot{s}_j^+ = i(2\epsilon_j + \omega) s_j^+ - 2i\bar{b} s_j^z \quad (5)$$

$$\dot{s}_j^- = -i(2\epsilon_j + \omega) s_j^- + 2i b s_j^z \quad (6)$$

Integrability is revealed after introducing the Lax matrices:

$$L(\lambda) = 2\lambda\sigma^z + 2(b\sigma^+ + \bar{b}\sigma^-) + \sum_{j=1}^n \frac{\vec{s}_j \cdot \vec{\sigma}}{\lambda - \epsilon_j} \quad (7)$$

$$M(\lambda) = -i\lambda\sigma^z - i\frac{\omega}{2}\sigma^z - i(b\sigma^+ + \bar{b}\sigma^-) \quad (8)$$

where σ^a are the Pauli matrices, $\sigma^\pm = \frac{1}{2}(\sigma^x \pm i\sigma^y)$.

$$\sigma^x = \begin{pmatrix} 0 & 1 \\ 1 & 0 \end{pmatrix}, \quad \sigma^y = \begin{pmatrix} 0 & -i \\ i & 0 \end{pmatrix}, \quad \sigma^z = \begin{pmatrix} 1 & 0 \\ 0 & -1 \end{pmatrix},$$

It is not difficult to check that the equations of motion are equivalent to the Lax equation:

$$\dot{L}(\lambda) = [M(\lambda), L(\lambda)] \quad (9)$$

Letting

$$L(\lambda) = \begin{pmatrix} A(\lambda) & B(\lambda) \\ C(\lambda) & -A(\lambda) \end{pmatrix}$$

we have:

$$A(\lambda) = 2\lambda + \sum_{j=1}^n \frac{s_j^z}{\lambda - \epsilon_j} \quad (10)$$

$$B(\lambda) = 2b + \sum_{j=1}^n \frac{s_j^-}{\lambda - \epsilon_j} \quad (11)$$

$$C(\lambda) = 2\bar{b} + \sum_{j=1}^n \frac{s_j^+}{\lambda - \epsilon_j} \quad (12)$$

These generating functions have the simple Poisson brackets:

$$\{L_1(\lambda), L_2(\mu)\} = -i \left[\frac{P_{12}}{\lambda - \mu}, L_1(\lambda) + L_2(\mu) \right]$$

where

$$P_{12} = \begin{pmatrix} 1 & 0 & 0 & 0 \\ 0 & 0 & 1 & 0 \\ 0 & 1 & 0 & 0 \\ 0 & 0 & 0 & 1 \end{pmatrix}$$

It follows immediately that $\text{Tr}(L^2(\lambda)) = 2A^2(\lambda) + 2B(\lambda)C(\lambda)$ Poisson commute for different values of the spectral parameter:

$$\{\text{Tr}(L^2(\lambda_1)), \text{Tr}(L^2(\lambda_2))\} = 0$$

Hence

$$\Lambda(\lambda) \equiv \frac{1}{2} \text{Tr}(L^2(\lambda)) = A^2(\lambda) + B(\lambda)C(\lambda)$$

generates Poisson commuting quantities. One has

$$\Lambda(\lambda) = \frac{Q_{2n+2}(\lambda)}{\prod_j (\lambda - \epsilon_j)^2} = 4\lambda^2 + 4H_{n+1} + 2 \sum_{j=1}^n \frac{H_j}{\lambda - \epsilon_j} + \sum_{j=1}^n \frac{s^2}{(\lambda - \epsilon_j)^2} \quad (13)$$

where $Q_{2n+1}(\lambda)$ is a polynomial of degree $2n + 2$. The $(n + 1)$ commuting Hamiltonians H_j , $j = 1, \dots, n + 1$ read:

$$H_{n+1} = b\bar{b} + \sum_{j=1}^n s_j^z \quad (14)$$

and

$$H_j = 2\epsilon_j s_j^z + (bs_j^+ + \bar{b}s_j^-) + \sum_{k \neq j} \frac{s_j \cdot s_k}{\epsilon_j - \epsilon_k}, \quad j = 1, \dots, n \quad (15)$$

The physically interesting Hamiltonian eq.(1) is:

$$H = \omega H_{n+1} + \sum_{j=1}^n H_j \quad (16)$$

On the physical phase space the complex conjugation acts as $\overline{s_j^z} = s_j^z$ and $\overline{s_j^+} = s_j^-$, and of course \bar{b} is the complex conjugate of b . Hence for λ real, $A(\lambda)$ is real and $B(\lambda) = \overline{C(\lambda)}$. It follows that on the physical phase space, $Q_{2n+2}(\lambda)$ is *positive* when λ is *real*.

2.2 Separated variables.

The Lax form eq. (9) of the equation of motion implies that the so-called spectral curve Γ , defined by $\det(L(\lambda) - \mu) = 0$ is a constant of motion. Specifically:

$$\Gamma : \mu^2 - A^2(\lambda) - B(\lambda)C(\lambda) = 0, \text{ i.e. } \mu^2 = \frac{Q_{2n+2}(\lambda)}{\prod_j (\lambda - \epsilon_j)^2} \quad (17)$$

Defining $y = \mu \prod_j (\lambda - \epsilon_j)$, the equation of the curve becomes $y^2 = Q_{2n+2}(\lambda)$ which is an hyperelliptic curve. Since the polynomial $Q_{2n+2}(\lambda)$ has degree $2n + 2$, the genus of the curve is n . Because the model is integrable, it is possible to construct action-angle coordinates (at least locally), but their connection to the initial physical dynamical variables is rather complicated. In this work, we preferred to work with the so-called separated variables which have the double advantage that their equations of motion are much simpler than the original ones and that they are not too far from the physical spin and oscillator coordinates. The separated variables are $g = n$ points on the curve whose coordinates (λ_k, μ_k) can be taken as coordinates on phase space. They are defined as follows. Let us write

$$C(\lambda) = 2\bar{b} + \sum_{j=1}^n \frac{s_j^+}{\lambda - \epsilon_j} \equiv 2\bar{b} \frac{\prod_{k=1}^n (\lambda - \lambda_k)}{\prod_{j=1}^n (\lambda - \epsilon_j)} \quad (18)$$

the separated coordinates are the collection $(\lambda_k, \mu_k = A(\lambda_k))$. They have canonical Poisson brackets

$$\{\lambda_k, \mu_{k'}\} = -i\delta_{k,k'}$$

Notice however that if $\bar{b} = 0$ these variables are not well defined.

There are only $2n$ such coordinates which turn out to be invariant under the global $U(1)$ rotation generated by H_{n+1} :

$$b \rightarrow e^{i\theta} b, \quad \bar{b} \rightarrow e^{-i\theta} \bar{b}, \quad s_j^- \rightarrow e^{i\theta} s_j^-, \quad s_j^+ \rightarrow e^{-i\theta} s_j^+$$

So they describe the *reduced* model obtained by fixing the value of H_{n+1} and taking into consideration only the dynamical variables invariant under this $U(1)$ action. The initial dynamical model can be recovered by adding the phase of the oscillator coordinates \bar{b}, b to the separated variables. The equations of motion with respect to H_i in these new variables are (no summation over k):

$$\partial_{t_i} \lambda_k = i\mu_k (\mathcal{B}^{-1})_{ik}, \quad \mathcal{B}_{kj} = \frac{1}{\lambda_k - \epsilon_j}, \quad (\mathcal{B}^{-1})_{jp} = \frac{\prod_{l \neq p} (\epsilon_j - \lambda_l) \prod_i (\lambda_p - \epsilon_i)}{\prod_{i \neq j} (\epsilon_j - \epsilon_i) \prod_{l \neq p} (\lambda_p - \lambda_l)} \quad (19)$$

Using the identities:

$$\sum_{i=1}^n \frac{\epsilon_i^p}{\prod_{j \neq i} (\epsilon_i - \epsilon_j)} = \delta_{p, n-1}, \quad 0 \leq p \leq n-1$$

the flow associated to the physical Hamiltonian eq.(16) reads:

$$\partial_t \lambda_k = i\mu_k \frac{\prod_j (\lambda_k - \epsilon_j)}{\prod_{l \neq k} (\lambda_k - \lambda_l)}, \quad \mu_k = A(\lambda_k) \quad (20)$$

The equations of motion eq.(20) must be complemented by the equation of motion for \bar{b}, b which allows to recover the motion of the full model from the motion of the separated variables in the reduced model. We have:

$$\partial_t \bar{b} = i\omega \bar{b} + i \sum_{\text{Res } \epsilon_j} C(\lambda) = i\omega \bar{b} - i \sum_{\text{Res } \infty} C(\lambda) = i\bar{b}(\omega - 2(\Sigma_1 - \sigma_1(\epsilon))) \quad (21)$$

where $\Sigma_1 = \sum_i \lambda_i$ and $\sigma_1(\epsilon) = \sum_i \epsilon_i$. Of course, we also have the complex conjugated equation of motion for b .

We show now how to reconstruct spin coordinates from the separated variables (λ_k, μ_k) and the oscillator coordinates (\bar{b}, b) . For $C(\lambda)$ we have eq.(18). It is a rational fraction of λ which has simple poles at $\lambda = \epsilon_j$ whose residue is s_j^+ . For $A(\lambda)$, we write:

$$A(\lambda) = \frac{P_{n+1}(\lambda)}{\prod_{j=1}^n (\lambda - \epsilon_j)}$$

The polynomial $P_{n+1}(\lambda) - 2\lambda \prod_{j=1}^n (\lambda - \epsilon_j)$ is of degree $n - 1$, and we know its value at the n points λ_j because:

$$P_{n+1}(\lambda_j) = \mu_j \prod_{k=1}^n (\lambda_j - \epsilon_k) \quad (22)$$

Therefore, we can write:

$$P_{n+1}(\lambda) = 2\lambda \prod_{j=1}^n (\lambda - \epsilon_j) + \sum_i (\mu_i - 2\lambda_i) \prod_{k=1}^n (\lambda_i - \epsilon_k) \frac{\prod_{l \neq i} (\lambda - \lambda_l)}{\prod_{l \neq i} (\lambda_i - \lambda_l)} \quad (23)$$

Once $A(\lambda)$ and $C(\lambda)$ are known, we can find the spin themselves by taking the residues at $\lambda = \epsilon_j$. We get:

$$s_j^+ = 2\bar{b} \frac{\prod_{i=1}^n (\epsilon_j - \lambda_i)}{\prod_{k \neq j}^n (\epsilon_j - \epsilon_k)}, \quad s_j^z = \frac{\prod_{l=1}^n (\epsilon_j - \lambda_l)}{\prod_{k \neq j}^n (\epsilon_j - \epsilon_k)} \sum_i \left[(2\lambda_i - \mu_i) \frac{\prod_{k \neq j} (\lambda_i - \epsilon_k)}{\prod_{l \neq i} (\lambda_i - \lambda_l)} \right] \quad (24)$$

The modulus of b is invariant under the global $U(1)$ action generated by H_{n+1} and is obtained from (recall that in the reduced model H_{n+1} is a parameter)

$$\bar{b}b = H_{n+1} - \sum_j s_j^z$$

The phase of b and \bar{b} is not determined in the reduced model. The same phase appears in the formula for s_j^+ . Finally, the s_j^- components are obtained from the constraints:

$$(s_i^z)^2 + s_i^+ s_i^- = s^2$$

They are determined up to the phase of $1/\bar{b}$.

Note that if the λ_i 's are arbitrary complex numbers, s_j^- is not the complex conjugate of s_j^+ , as it is the case for the physical phase-space. This shows that separated variables are natural coordinates on the *complexified* phase-space. In these variables, the problem of identifying the sets $\{\lambda_i, \mu_i\}$ corresponding to physical configurations (i.e. those for which all spin components are real) is rather non-trivial, and most of the present work is dedicated to it.

In many situations, and in particular in this article, we are interested in the system with prescribed real values of the conserved quantities, H_1, \dots, H_{n+1} , i.e. we take as coordinates the (λ_j, H_j) instead of the (λ_j, μ_j) . This amounts to fixing the Liouville torus we work with, or equivalently the spectral polynomial $Q_{2n+2}(\lambda)$. In this setting, the μ_j are determined by the equation

$$\prod_{k=1}^n (\lambda_j - \epsilon_k) \mu_j = \pm \sqrt{Q_{2n+2}(\lambda_j)}$$

The choice of the signs in this formula is very important and will be a recurrent theme in our subsequent discussions. They affect the formulae for s_j^z or equivalently the polynomial $P_{n+1}(\lambda)$. The values of s_j^- 's can then be obtained from $B(\lambda)$ which is determined by:

$$B(\lambda) = \frac{Q_{2n+2}(\lambda) - P_{n+1}^2(\lambda)}{C(\lambda) \prod_k (\lambda - \epsilon_k)^2} = \frac{1}{2b} \frac{Q_{2n+2}(\lambda) - P_{n+1}^2(\lambda)}{\prod_i (\lambda - \lambda_i) \prod_k (\lambda - \epsilon_k)} \quad (25)$$

The polynomial in the numerator is of degree $2n$, and moreover it is divisible by $\prod_i (\lambda - \lambda_i)$ because $P_{n+1}^2(\lambda_i) = Q_{2n+2}(\lambda_i)$, so we can write

$$B(\lambda) = 2b \frac{\prod_i (\lambda - \bar{\lambda}_i)}{\prod_k (\lambda - \epsilon_k)} \quad (26)$$

The spin components s_j^- are obtained by taking the residue at $\lambda = \epsilon_j$:

$$s_j^- = 2b \frac{\prod_i (\epsilon_j - \bar{\lambda}_i)}{\prod_{k \neq j} (\epsilon_j - \epsilon_k)}$$

In this construction, the variables $\bar{\lambda}_i$ and the corresponding $\bar{\mu}_i$ are complicated functions of the (λ_i, H_i) and of the choice of signs used in the determination of the variables μ_i . The set of physical configurations (often referred to here as the *real slice*) is obtained by writing that the set $(\bar{\lambda}_i, \bar{\mu}_i)$ is the *complex conjugate* of the set (λ_i, μ_i) . This leads to a set of complicated relations whose solution is not known in general. It is the purpose of this work to show how to implement them in particular cases.

2.3 Moment map and degenerate spectral curves

In this section, we discuss the case of a spectral polynomial having double roots, so that $Q_{2n+2}(\lambda)$ can be written as:

$$Q_{2n+2}(\lambda) = 4 p_{2m+2}(\lambda) \prod_{i=1}^{n-m} (\lambda - E_i)^2, \quad p_{2m+2}(\lambda) = \lambda^{2m+2} + b_{2m+1} \lambda^{2m+1} + \dots \quad (27)$$

The E_i are either real or come in complex conjugated pairs. Moreover $p_{2m+2}(\lambda)$ is positive for real λ . As discussed in some previous works [5, 11, 16], this corresponds to critical values of the moment map. The preimage of the moment map for such value is a stratified manifold, whose various strata have dimensions ranging from $m + 1$ to $n + 1$. Separated variables provide a very natural access to this stratification, because each stratum of dimension $n - n_0 + 1$ can be obtained by freezing $n_0 \leq n - m$ separated variables λ_j^0 on n_0 double zeroes of $Q_{2n+2}(\lambda)$. On such stratum, the rank of the moment map also drops to $n - n_0 + 1$. As explained before [5], the dynamics of the system for initial conditions lying in this stratum is very similar to the one of an effective model with $n - n_0$ spins, but we shall not use this physically appealing result here.

To produce a polynomial $Q_{2n+2}(\lambda)$ of the form eq.(27) is not completely straightforward because it must also be compatible with eq.(13). Let us explain how it works.

The fact that the rational fraction $Q_{2n+2}(\lambda)/\prod_j(\lambda - \epsilon_j)^2$ has double poles at $\lambda - \epsilon_j$ whose weight is s^2 imposes n conditions:

$$\prod_i (\lambda - E_i)|_{\epsilon_j} = \frac{s\alpha_j}{2\sqrt{p_{2m+2}(\epsilon_j)}} \prod_{k \neq j} (\epsilon_j - \epsilon_k)$$

where $\alpha_j = \pm 1$. The values of the polynomial $\prod_i(\lambda - E_i)$ at the n points ϵ_j are therefore known, and we can write by Lagrange interpolation formula:

$$\prod_i (\lambda - E_i) = \sum_j \frac{s\alpha_j}{2\sqrt{p_{2m+2}(\epsilon_j)}} \prod_{i \neq j} (\lambda - \epsilon_i) \quad (28)$$

But the degree of the left hand side is $n - m$ while the degree on the right hand side is superficially $n - 1$, so we have the consistency conditions:

$$\sum_j \frac{\alpha_j \epsilon_j^k}{2\sqrt{p_{2m+2}(\epsilon_j)}} = 0, \quad k = 0, \dots, m - 2 \quad (29)$$

and:

$$\sum_j \frac{s\alpha_j \epsilon_j^{m-1}}{2\sqrt{p_{2m+2}(\epsilon_j)}} = 1 \quad (30)$$

These equations are obtained by writing that:

$$\oint \frac{dz}{2\pi i} \frac{z^k \prod_{i=1}^{n-m} (z - E_i)}{\prod_{i=1}^n (z - \epsilon_i)} = \delta_{k,m-1}, \quad k = 0, \dots, m - 1$$

where the integrals are taken along a contour in the complex plane which encircles all the ϵ_j 's. These are exactly m conditions on the $2m + 3$ coefficients of $p_{2m+2}(\lambda)$, of which the leading coefficient is known. One more condition is obtained by writing that in the right-hand side of eq. (13) the coefficient of λ vanishes. This gives:

$$b_{2m+1} + 2(\sigma_1(\epsilon) - \sigma_1(E)) = 0$$

But we also have:

$$\oint \frac{dz}{2\pi i} \frac{z^m \prod_{i=1}^{n-m} (z - E_i)}{\prod_{i=1}^n (z - \epsilon_i)} = \sigma_1(\epsilon) - \sigma_1(E) = \sum_j \frac{s\alpha_j \epsilon_j^m}{2\sqrt{p_{2m+2}(\epsilon_j)}}$$

where the integral is again on a contour encircling all the ϵ_j 's. Assembling the previous two equations gives the consistency condition:

$$b_{2m+1} + \sum_j \frac{s\alpha_j \epsilon_j^m}{\sqrt{p_{2m+2}(\epsilon_j)}} = 0 \quad (31)$$

Altogether, we are left with $m + 1$ free coefficients in $p_{2m+2}(\lambda)$ which play the role of conserved Hamiltonians of an effective system with m spins [5]. All the other symmetric functions $\sigma_k(E)$, $k > 1$ are then determined by eq.(28).

If $m = -1$, that is to say $p_{2m+2}(\lambda) = 1$, eq.(28) must be slightly modified as

$$\prod_i (\lambda - E_i) = (\lambda + \beta) \prod_j (\lambda - \epsilon_j) + \sum_j \frac{s\alpha_j}{2} \prod_{i \neq j} (\lambda - \epsilon_i) \quad (32)$$

This means

$$\frac{Q_{2n+2}(\lambda)}{\prod_j (\lambda - \epsilon_j)^2} = \left(2\lambda + 2\beta + \sum_j \frac{\alpha_j s}{\lambda - \epsilon_j} \right)^2 \quad (33)$$

Comparing with eq.(13) at $\lambda = \infty$ we see that $\beta = 0$.

Let us discuss now the freezing of the λ_k at the double roots of $Q_{2n+2}(\lambda)$. The equations of motion eq.(20) become

$$\partial_t \lambda_k = \pm i \frac{\prod_j (\lambda_k - E_j) \sqrt{p_{2m+2}(\lambda_k)}}{\prod_{l \neq k} (\lambda_k - \lambda_l)}, \quad (34)$$

so if $\lambda_k = E_i$ at $t = 0$, it stays there forever, and it is consistent with the equations of motion to freeze some λ_k at the double roots of $Q_{2n+2}(\lambda)$. This however cannot be done in an arbitrary way as we now explain.

Let us assume that $Q_{2n+2}(\lambda)$ has a *real* root at $\lambda = E$. This means that $A^2(\lambda) + B(\lambda)C(\lambda)$ vanishes when $\lambda = E$. But for real λ , $A(\lambda)$ is real and one has $C(\lambda) = \overline{B(\lambda)}$ so that $A(\lambda)$, $B(\lambda)$, $C(\lambda)$ must all vanish at $\lambda = E$. In particular, recalling eq.(18), this means that one of the separated variables, say λ_1 , is frozen at the value E , *provided* $\bar{b}b \neq 0$. This implies also that $\lambda - E$ divides simultaneously $A(\lambda)$, $B(\lambda)$ and $C(\lambda)$, and therefore $(\lambda - E)^2$ divides $Q_{2n+2}(\lambda)$. A single real root of $Q_{2n+2}(\lambda)$ is necessarily a double root. Writing: $A(\lambda) = (\lambda - E)\tilde{A}(\lambda)$, $B(\lambda) = (\lambda - E)\tilde{B}(\lambda)$, $C(\lambda) = (\lambda - E)\tilde{C}(\lambda)$, $Q_{2n+2}(\lambda) = (\lambda - E)^2\tilde{Q}_{2n}(\lambda)$, we see that:

$$\tilde{Q}_{2n}(\lambda) = \prod_j (\lambda - \epsilon_j)^2 \left(\tilde{A}(\lambda)^2 + \tilde{B}(\lambda)\tilde{C}(\lambda) \right)$$

so we can apply the same discussion to the real roots of $\tilde{Q}_{2n}(\lambda)$. We deduce from this that the multiplicity p of the real root E of $Q_{2n+2}(\lambda)$ is even and that $(\lambda - E)^{p/2}$ divides simultaneously $A(\lambda)$, $B(\lambda)$ and $C(\lambda)$. In this case, $p/2$ separated variables $\lambda_1, \dots, \lambda_{p/2}$ are frozen at the real value E .

Nothing as simple holds in the case of a simple *complex* root. So, let us assume that there is a *double* complex root E . Of course the complex conjugate \bar{E} is also a double root. What can be said in general is that the values of $\lambda_1, \dots, \lambda_n$ freeze by complex conjugated pairs.

In fact we have $\Lambda(\lambda) = A^2(\lambda) + B(\lambda)C(\lambda)$ hence

$$\Lambda'(\lambda) = 2A(\lambda)A'(\lambda) + B'(\lambda)C(\lambda) + B(\lambda)C'(\lambda)$$

On a degenerate spectral curve, $\Lambda(\lambda)$ has at least one double zero E . Therefore

$$\begin{aligned} 0 &= A^2(E) + B(E)C(E) \\ 0 &= 2A(E)A'(E) + B'(E)C(E) + B(E)C'(E) \end{aligned}$$

By contrast to the real case, we cannot infer from these equations that $C(E) = 0$. This is related to the fact that for critical spectral curves associated to unstable critical points, the corresponding level set of the conserved Hamiltonians has dimension equal to the number of unstable modes. So we expect that some separated variables λ_j can remain unfrozen. But if one of them freezes at E , that is if $C(E) = 0$, the first equation implies $A(E) = 0$ and the second equation implies $B(E)C'(E) = 0$. Therefore if the zero of $C(\lambda)$ at $\lambda = E$ is simple, then necessarily $B(E) = 0$. But $B(E)$ is the complex conjugate of $C(\bar{E})$ which must therefore vanish *provided* $\bar{b}b \neq 0$. From this we conclude that another separated variable λ_k freezes at \bar{E} .

In contrast to the real case, freezing is not compulsory, but it is the possibility to freeze the λ_i by complex conjugated pairs that leads to the description of the real slice and the stratification of the level set.

3 The one-spin model.

The model with a single spin coupled to the oscillator is interesting, because it illustrates most of the points discussed so far. In this case, there are only two conserved quantities, H_1 and H_2 , which read:

$$H_1 = 2\epsilon_1 s_1^z + b s_1^\dagger + \bar{b} s_1^- \quad (35)$$

$$H_2 = \bar{b}b + s_1^z \quad (36)$$

The rank of the momentum map can be either 0, 1, or 2. The later case corresponds to generic Arnold-Liouville tori of dimension 2. Let us now recall briefly the discussion of critical values of the moment map given in a previous work [11].

3.1 Rank zero

The rank of the moment map vanishes on the critical points given by $b = \bar{b} = 0, s_1^\pm = 0$. Hence we have two points:

$$s_1^z = e_1 s, \quad e_1 = \pm 1$$

The corresponding values $P = (H_1, H_2)$ are:

$$P_1(\uparrow) = [2\epsilon_1 s, s], \quad P_2(\downarrow) = [-2\epsilon_1 s, -s]$$

To determine the type of the singularities, we look at the classical Bethe equations (see section 9) which read:

$$2E + \frac{se_1}{E - \epsilon_1} = 0 \Leftrightarrow 2E^2 - 2\epsilon_1 E + se_1 = 0$$

The discriminant of this equation is $\epsilon_1^2 - 2se_1$. When the spin is down (point $P_2(\downarrow)$), the discriminant is positive, the two classical Bethe roots are real and this is an elliptic singularity, in agreement with the general analysis of section 9. When the spin is up (point $P_1(\uparrow)$) we have real roots when $\epsilon_1^2 \geq 2s$ (i.e. the singularity is elliptic in this case), and a pair of complex conjugate roots E, \bar{E} when $\epsilon_1^2 \leq 2s$ (i.e. the singularity is focus-focus in that case). The image of the moment map is shown on Fig.[2] in the unstable case. We see that the stable critical point $P_1(\uparrow)$ is located at the tip of the image of the moment map, whereas the unstable one $P_2(\downarrow)$ lies in the interior of this domain.

In the one spin case, eq.(13) reads :

$$\frac{Q_4(\lambda)}{(\lambda - \epsilon_1)^2} = 4\lambda^2 + 4H_2 + 2\frac{H_1}{\lambda - \epsilon_1} + \frac{s^2}{(\lambda - \epsilon_1)^2} \quad (37)$$

For the values $H_1 = 2\epsilon_1 e_1 s, H_2 = e_1 s$ it is completely degenerate and the spectral polynomial has two double roots E_1, E_2 identical to the classical Bethe roots, and reads:

$$Q_4(\lambda) = 4(\lambda^2 - \epsilon_1 \lambda + \frac{s}{2} e_1)^2 = 4(\lambda - E_1)^2 (\lambda - E_2)^2$$

where

$$E_1 + E_2 = \epsilon_1, \quad E_1 E_2 = \frac{se_1}{2}$$

Let us now describe in more detail the real slices corresponding to the two critical values of (H_1, H_2) . Recall that

$$s_1^z = (\epsilon_1 - \lambda_1)(2\lambda_1 - \mu_1) \quad (38)$$

We express first the separated variable μ_1 as a function of λ_1 :

$$\mu_1 = \pm 2 \frac{(\lambda_1 - E_1)(\lambda_1 - E_2)}{(\lambda_1 - \epsilon_1)} \quad (39)$$

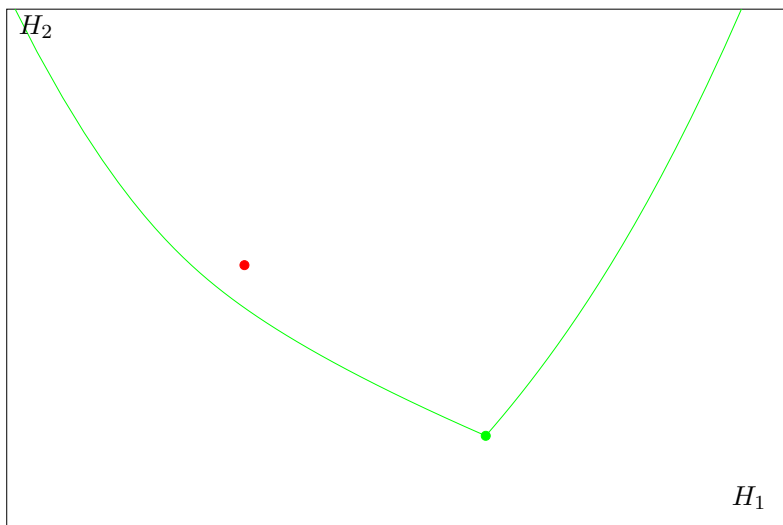


Figure 2: The image of the moment map in the case of one spin, ($\epsilon_1 = -0.707$), with one unstable critical point. The green point is the stable (elliptic) point $P_2(\downarrow)$. The red point is the unstable (focus-focus) point $P_1(\uparrow)$. It is in the interior of the image of the moment map. The two boundaries of this domain correspond to spectral polynomials which one double real zero, so that the moment map has rank 1 on the preimage of these curves.

We have to distinguish the stable and unstable cases. In the stable case E_1 and E_2 are real and we know that λ_1 has to be frozen at one of them, say E_1 . Then $\mu_1 = 0$, there is no problem of sign in eq.(39) and

$$s_1^z = 2E_1(\epsilon_1 - E_1) = 2E_1E_2 = se_1$$

as it should be. The level set in this case is composed of only one stratum consisting of the critical point itself where the rank of the moment map is zero.

Let us now assume that we are in the unstable case, that is at the point $P_2(\uparrow)$, $e_1 = +1$ and $2s - \epsilon_1^2 \geq 0$. In this case $E_1 = E, E_2 = \bar{E}$ are complex and λ_1 remains unfrozen. Let us choose the + sign in eq.(39). Inserting into eq.(38) we obtain

$$s_1^z = se_1$$

so that, in the spin variables, we are precisely at the critical point. On this stratum of the level set the rank of the moment map is zero. It is very interesting to remark that the variable λ_1 completely disappears in this case (hence the rank zero). In terms of the separated variable, this

stratum of the level set seems therefore to consist of the whole λ_1 -plane. This is due to the fact that at the critical point $\bar{b}b = 0$ and the separated variables are not well defined and appear as singular coordinates. However, as we will show below, the λ_1 coordinate has the magic property of realizing a blowup of the singularity.

Choosing now the $-$ sign in eq. (39) yields:

$$s_1^z = -se_1 - 4\lambda_1(\lambda_1 - \epsilon_1)$$

Writing that s_1^z is real, $s_1^z = \bar{s}_1^z$, gives

$$\lambda_1 + \bar{\lambda}_1 = \epsilon_1 \quad (40)$$

Setting $\lambda_1 = x + iy$, $\bar{\lambda}_1 = x - iy$, we see that the real slice is given by the vertical line located at $x = \epsilon_1/2$. It is not the whole line however. We find from $\bar{b}b = H_2 - s_1^z$

$$\bar{b}b = 2s - \epsilon_1^2 - 4y^2 \geq 0$$

The real slice of the reduced model corresponds in this case to the segment parallel to the imaginary axis delimited by the two double roots E and \bar{E} of the spectral polynomial. This manifold has real dimension one.

As we have discussed before [11, 18], this corresponds to a real slice of the model reduced by the global $U(1)$ action eq.(21). From the viewpoint of the original model, we have to reintroduce this global angle and the real slice becomes a two dimensional torus pinched at the unstable critical point.

Hence in this simple case we see that the level set of the unstable critical point is composed of two strata : the critical point itself where the rank of the moment map is zero and the pinched torus where the rank is two.

The dynamics of the model on this torus is the composition of a large motion in which the oscillator amplitude $\bar{b}b$ goes to zero at time $\pm\infty$ but reaches a finite maximum at a finite time, and a global $U(1)$ rotation. Only the former movement is captured by the reduced model, and it maps into the finite segment of the λ_1 variable which we have just described. To see this, let us consider the equation of motion for the flow generated by H_1 :

$$\partial_{t_1} \lambda_1 = 2i(\lambda_1 - E)(\lambda_1 - \bar{E}) \quad (41)$$

whose solution is:

$$\lambda_1 = \frac{E - \bar{E}X}{1 - X}, \quad X = X_0 e^{2i(E - \bar{E})t_1} \quad (42)$$

The reality condition eq.(40) becomes:

$$(E - \bar{E})(X - \bar{X}) = 0$$

which imposes $\bar{X}_0 = X_0$ so that X_0 is real. Its absolute value can be absorbed in the origin of time t_1 . Only its sign matters. The constraint $s_1^z \leq s$ is equivalent to $X_0 < 0$, and we recover the fact that λ_1 runs along the line interval joining E and \bar{E} .

3.2 Rank one

Physical configurations at which the rank of the moment map is equal to one correspond to a spectral polynomial with one double zero, which is necessarily real. We therefore write:

$$Q_4(\lambda) = (\lambda + a_0)^2(b_2\lambda^2 + b_1\lambda + b_0) \quad (43)$$

where a_0 and b_i are real. We denote:

$$a_0 = \frac{1}{2}x - \epsilon_1$$

Taking into account the usual constraints on $Q_4(\lambda)$ saying that it depends only on two free parameters H_1 and H_2 , see eq.(37), we can determine b_0 , b_1 , and b_2 in terms of x by solving linear equations. We find:

$$\begin{aligned} b_2 = 4, \quad b_1 = -4x, \quad b_0 = 4 \frac{\epsilon_1 x^3 - \epsilon_1^2 x^2 + s^2}{x^2} \\ H_1 = -\frac{x^4 - 2\epsilon_1 x^3 - 4s^2}{2x} \\ H_2 = -\frac{3x^4 - 8\epsilon_1 x^3 + 4\epsilon_1^2 x^2 - 4s^2}{4x^2} \end{aligned}$$

These are parametric equations for a curve which coincides with the boundaries of the image of the moment map in the (H_1, H_2) plane, for which an illustration can be found on Fig.[2].

The determination of the real slice is straightforward in this case. Indeed, because we have a real double root, the separated variable is frozen at the value $\lambda_1 = -a_0, \mu_1 = 0$. This single point of the reduced model corresponds to the one-dimensional orbits under the global rotations generated by H_2 characterized by a common phase on \bar{b} and s_1^+ :

$$\begin{aligned} s_1^z &= -\frac{1}{2}x(x - 2\epsilon_1) \\ \bar{b}b &= \frac{(2s - x^2 + 2\epsilon_1 x)(2s + x^2 - 2\epsilon_1 x)}{4x^2} \\ s_1^+ &= x\bar{b} \end{aligned}$$

Hence, we have shown that the preimage of a point on the boundary consists of only one stratum which is a circle S^1 . Notice that when

$$x^2 - 2\epsilon_1 x + 2es = 0, \quad e = \pm 1 \quad (44)$$

we have $s_1^z = es$ and $\bar{b}b = 0$ and this corresponds to the points $P_1(\downarrow)$ and $P_2(\uparrow)$.

In fact there is a simple relation between rank 0 and rank 1. The spectral curves eq.(43) degenerate when the polynomial $b_2\lambda^2 + b_1\lambda + b_0$ has a double real root. Its discriminant is:

$$b_1^2 - 4b_0b_2 = 16 \frac{(x^2 - 2\epsilon_1 x - 2s)(x^2 - 2\epsilon_1 x + 2s)}{x^2} = -64 \bar{b}b \leq 0$$

It vanishes precisely when eqs.(44) are satisfied. These equations are nothing but the classical Bethe equations eq.(109) as can be seen by setting $x = 2E$. Hence in the stable case, the discriminant vanishes for real values of x , and the critical points are on the boundary lines of rank one. In the unstable case however the discriminant vanishes for complex values of x and the critical point cannot lie on the boundary.

3.3 Reality conditions on a generic torus.

In this simple case of a single spin it turns out that one can work out explicitly the exact reality conditions, for an arbitrary choice of the conserved quantities H_1 and H_2 . For this, express everything in terms of λ_1 and $\bar{\lambda}_1$. First, we have

$$s_1^+ = 2\bar{b}(\epsilon_1 - \lambda_1), \quad s_1^- = 2b(\epsilon_1 - \bar{\lambda}_1),$$

In the reduced model, H_2 is a constant and we have

$$(H_2 - \bar{b}b)^2 = (s_1^z)^2 = s^2 - s_1^+ s_1^-$$

which yields

$$(\bar{b}b)^2 + (4X - 2H_2)\bar{b}b + H_2 - s^2 = 0$$

where $X = (\lambda_1 - \epsilon_1)(\bar{\lambda}_1 - \epsilon_1)$. Finally eqs.(35) and (36) give:

$$H_1 = 2\epsilon_1 H_2 - 2\bar{b}b(\lambda_1 + \bar{\lambda}_1 - \epsilon), \quad (45)$$

Eliminating $\bar{b}b$ between these two equations, we get :

$$\begin{aligned} R : & (H_1 - 2\epsilon_1 H_2)^2 + 4(H_1 - 2\epsilon_1 H_2)(\lambda_1 + \bar{\lambda}_1 - \epsilon_1)(H_2 - 2\lambda_1 \bar{\lambda}_1 + 2\epsilon_1(\lambda_1 + \bar{\lambda}_1 - \epsilon_1)) \\ & + 4(H_2^2 - s^2)(\lambda_1 + \bar{\lambda}_1 - \epsilon_1)^2 = 0 \end{aligned} \quad (46)$$

To obtain the equation of the real slice we ask that λ_1 and $\bar{\lambda}_1$ are mutually complex conjugates. Setting $\lambda_1 = x + iy$, $\bar{\lambda}_1 = x - iy$, the expression R is quadratic in y and cubic in x . It can be uniformized by Weierstrass functions. Setting:

$$x = \frac{-6\epsilon_1 u + 10\epsilon_1 H_2 - 3H_1 - 2\epsilon_1^2}{4(-3u + 2H_2 - \epsilon_1^2)}, \quad y = \frac{-3v}{4(-3u + 2H_2 - \epsilon_1^2)}$$

the reality condition for λ_1 takes the standard form for a planar cubic:

$$v^2 = 4u^3 - g_2 u - g_3$$

with

$$g_2 = \frac{4}{3}(H_2^2 + 2\epsilon_1^2 H_2 - 3\epsilon_1 H_1 + \epsilon_1^4 + 3s^2)$$

$$g_3 = \frac{1}{27}(8H_2^3 + 24\epsilon_1^2 H_2^2 - 36\epsilon_1 H_1 H_2 - 72s^2 H_2 + 24\epsilon_1^4 H_2 + 27H_1^2 - 36\epsilon_1^3 H_1 + 36\epsilon_1^2 s^2 + 8\epsilon_1^6)$$

The range of physically acceptable values of x is determined by imposing:

$$\bar{b}b = -\frac{H_1 - 2\epsilon_1 H_2}{2(\lambda_1 + \bar{\lambda}_1 - \epsilon_1)} \geq 0, \text{ or } s_1^z = H_2 - \bar{b}b = H_2 + \frac{H_1 - 2\epsilon_1 H_2}{2(\lambda_1 + \bar{\lambda}_1 - \epsilon_1)} \in \{-s, +s\}$$

where we have used eq. (45).

To help visualize these real slices in the λ_1 complex plane, we consider a small circle around the image of the unstable point in the (H_1, H_2) plane:

$$H_1 = 2s\epsilon_1 + r \sin \theta, \quad H_2 = s + r \cos \theta \quad (47)$$

and we obtain a family of real slices shown in Fig.[3]. When $H_1 = 2\epsilon_1 H_2$, $H_2 \neq \pm s$, the reality condition eq.(46) simplifies to

$$\lambda_1 + \bar{\lambda}_1 - \epsilon_1 = 0 \quad (48)$$

In fact, on the line $H_1 = 2\epsilon_1 H_2$, the polynomial $Q_4(\lambda)$ depends on the variable $\lambda(\lambda - \epsilon_1)$ only which is invariant under the involution $\lambda \rightarrow \epsilon_1 - \lambda$. The slices thus become the vertical real line $x = \epsilon_1/2$ when $\theta = \theta_c$ where $\tan \theta_c = 2\epsilon_1$.

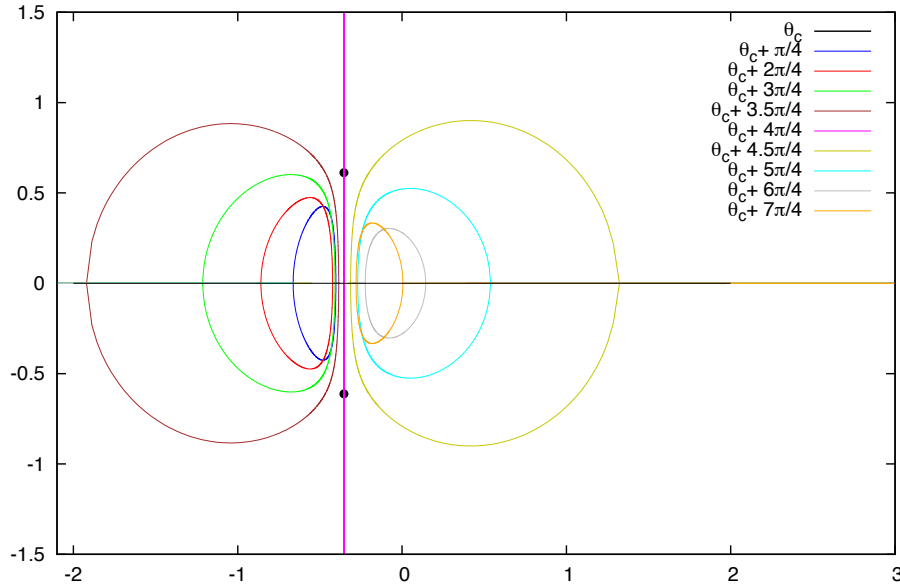


Figure 3: The real slices when we run around the small circle around the singularity. $\epsilon_1 = -0.707$, $r = 0.3$.

The two critical points lie on the line $H_1 = 2\epsilon_1 H_2$. When we are close to them,

$$H_1 = 2\epsilon_1 s e_1 + \delta H_1, \quad H_2 = s e_1 + \alpha \delta H_1$$

Keeping the first order term in eq.(46) we see that the real slice is the product of the straight line:

$$\lambda_1 + \bar{\lambda}_1 - \epsilon_1 = 0$$

by the circle:

$$(1 - 2\epsilon_1 \alpha)[2(\lambda_1 - \epsilon_1)(\bar{\lambda}_1 - \epsilon_1) - s e_1] - 2s e_1 \alpha (\lambda_1 + \bar{\lambda}_1 - \epsilon) = 0 \quad (49)$$

We can rewrite the above equation as:

$$(\lambda_1 - \lambda_\alpha)(\bar{\lambda}_1 - \lambda_\alpha) = (E_1 - \lambda_\alpha)(E_2 - \lambda_\alpha), \quad \lambda_\alpha = \epsilon_1 + \frac{\alpha s e_1}{1 - 2\epsilon_1 \alpha}$$

where E_i are the solutions of the classical Bethe equation:

$$2E(E - \epsilon_1) + s e_1 = 0$$

In the stable case $e_1 = -1$, the E_i are real and when α varies, we have a pencil of circles with limit points located at $\lambda_\alpha = E_1$ and $\lambda_\alpha = E_2$, see Fig.[4].

In the unstable case obtained when $e_1 = +1$ and $\epsilon_1^2 < 2s$, the E_i are complex conjugate to each other and we have a pencil of circles with base points located at $\lambda_\alpha = E$ and $\lambda_\alpha = \bar{E}$, see Fig.[5].

This expansion of eq. (46) gives a very reasonable approximation of the real slice for (H_1, H_2) close to the image of the unstable critical point $P_1(\uparrow)$ under the moment map. In Fig.[6], we see that for such values, the exact real slice is composed of two parts. One part is close to the vertical segment joining the two double roots E and \bar{E} of the spectral polynomial associated to $P_1(\uparrow)$. The second part is close to a circle belonging to the pencil just described. Here, we see a rather striking consequence of the fact that separated variables are singular in the vicinity of the critical points. Whereas the pinched torus containing the unstable critical point $P_1(\uparrow)$ appears as a *segment* of the vertical line eq.(48) in the λ_1 plane, any generic invariant torus arbitrary close to it is projected into a *closed curve*, whose shape depends crucially on the *direction* in the (H_1, H_2) plane along which we are approaching the critical value. The additional arc, well approximated by an element of the pencil of circles, corresponds to physical configurations which remain close to the unstable point $P_1(\uparrow)$. To establish this, it is useful to use the quadratic normal form of the moment map in the vicinity of $P_1(\uparrow)$ [11], whose construction is recalled in section 9.

3.4 Normal coordinates.

To study the vicinity of a critical point, we can use the normal coordinates defined in eq.(115). We have

$$C(\lambda) = \frac{2}{\lambda - \epsilon_1} \left[\left(\frac{C_1}{a'_1} + \frac{C_2}{a'_2} \right) \lambda - \left(\frac{C_1}{a'_1} E_2 + \frac{C_2}{a'_2} E_1 \right) \right]$$

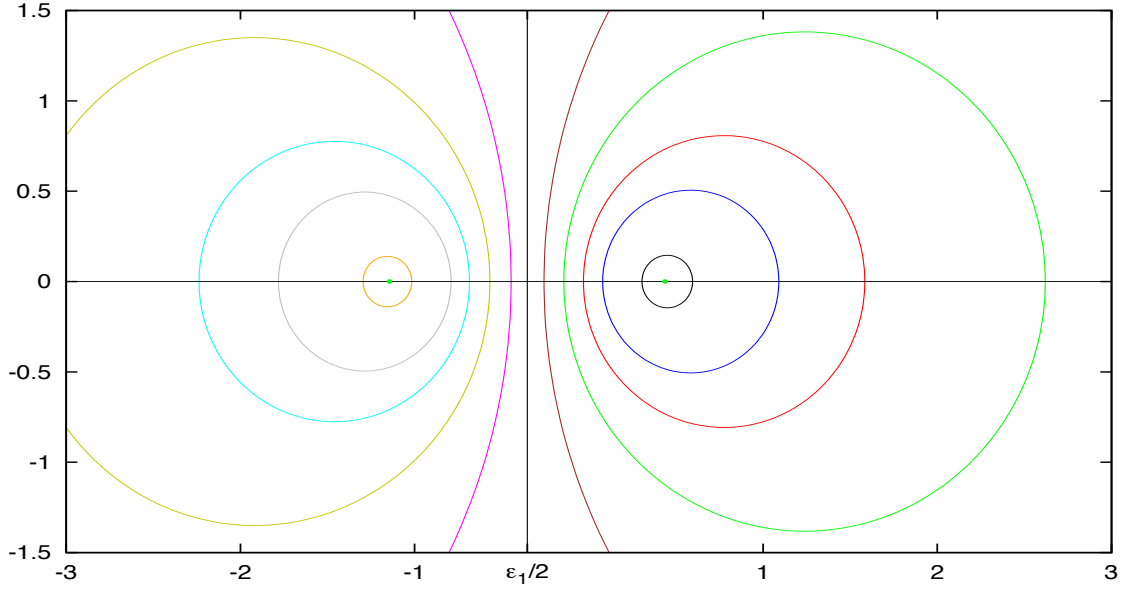


Figure 4: The pencil of circles in the stable case $\epsilon_1 = -0.707$

The zero of $C(\lambda)$ is the separated variable λ_1 . We have

$$\lambda_1 = \frac{E_2 a'_2 C_1 + E_1 a'_1 C_2}{a'_2 C_1 + a'_1 C_2} \quad (50)$$

It is important to remark that since λ_1 depends only on the ratio C_1/C_2 a small neighborhood of the critical point is mapped to the whole λ_1 plane.

We can parametrize the normal coordinates in terms of action-angle coordinates making explicit the reality conditions.

In the stable case, we set:

$$C_j = A_j e^{i\theta_j}, \quad B_j = A_j e^{-i\theta_j}$$

with real parameters A_j, θ_j . The real slice in the λ_1 variables is therefore given by:

$$\lambda_1(\theta) = \frac{E_2 a'_2 A_1 + E_1 a'_1 A_2 e^{i\theta}}{a'_2 A_1 + a'_1 A_2 e^{i\theta}}, \quad \theta = \theta_2 - \theta_1$$

Taking the complex conjugate, we can eliminate θ between λ_1 and $\bar{\lambda}_1$. We find:

$$(a'_1)^2 A_2^2 (\lambda_1 - E_1) (\bar{\lambda}_1 - E_1) - (a'_2)^2 A_1^2 (\lambda_1 - E_2) (\bar{\lambda}_1 - E_2) = 0$$

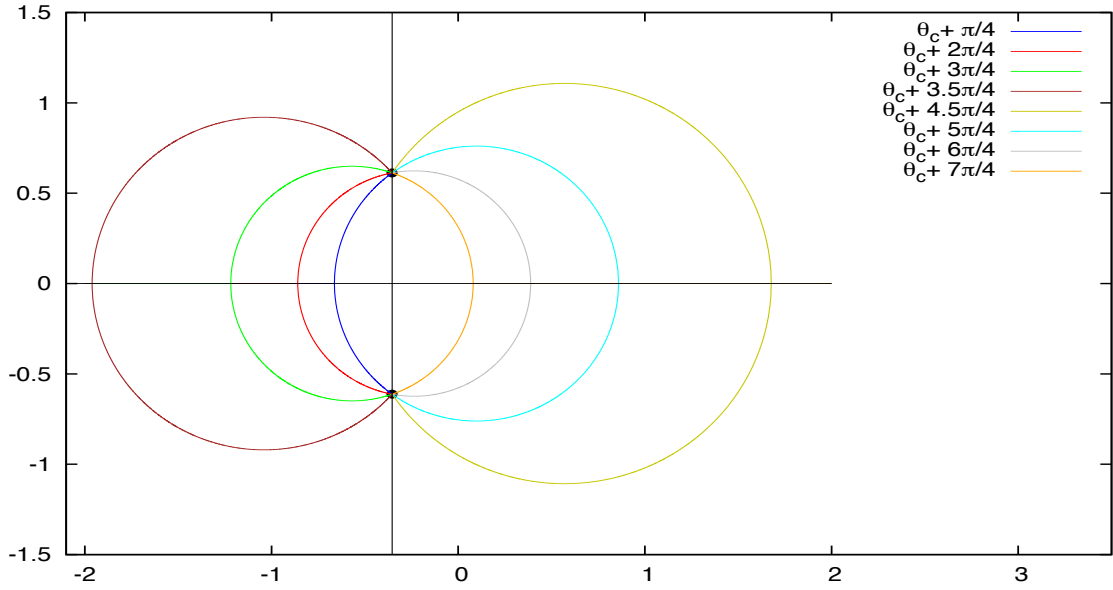


Figure 5: The pencil of circles in the stable case ($\epsilon_1 = -0.707$.)

and we recover our circle pencil with limit points E_1 and E_2 corresponding to $A_1 = 0$ and $A_2 = 0$ respectively.

In the unstable case, we set:

$$B_1 = A_1 \rho e^{i\theta}, \quad C_1 = A_1 \rho^{-1} e^{-i\theta}, \quad B_2 = \bar{A}_1 \rho^{-1} e^{i\theta}, \quad C_2 = \bar{A}_1 \rho e^{-i\theta}$$

where ρ is a real positive number. Then:

$$\lambda_1(\rho) = \frac{E_2 a'_2 A_1 + E_1 a'_1 \bar{A}_1 \rho^2}{a'_2 A_1 + a'_1 \bar{A}_1 \rho^2}$$

Taking the complex conjugate, remembering that $\bar{E}_1 = E_2$, we can eliminate ρ^2 and get:

$$(a'_1)^2 \bar{A}_1^2 (\lambda_1 - E_1) (\bar{\lambda}_1 - E_1) - (a'_2)^2 A_1^2 (\lambda_1 - E_2) (\bar{\lambda}_1 - E_2) = 0$$

This is a circle pencil with base points E_1 and E_2 .

The conserved quantities are given by:

$$H_2 = s + \frac{A_1^2}{2a'_1} + \frac{\bar{A}_1^2}{2a'_2}, \quad H_1 = 2s\epsilon_1 + \frac{sA_1^2}{2(\epsilon_1 - E_1)a'_1} + \frac{s\bar{A}_1^2}{2(\epsilon_1 - E_2)a'_2}$$

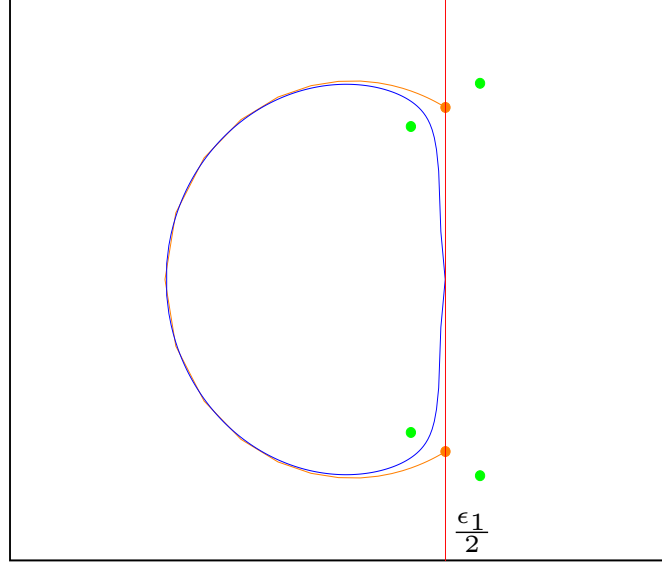


Figure 6: The exact real slice (in blue) compared to the corresponding circle (in orange) of the pencil in the unstable case. The green dots are the branch points of the spectral curve. The vertical line is the line $\lambda_1 + \bar{\lambda}_1 = \epsilon_1$. The orange points are the classical Bethe roots. ($\epsilon_1 = -0.707$, $H_1 = 2\epsilon_1 H_2 + 0.1$, $H_2 = 1$.)

so that using the parametrization eq.(47), the equation of the pencil becomes:

$$\sin \theta [2(\lambda_1 - \epsilon_1)(\bar{\lambda}_1 - \epsilon_1) - s] - 2 \cos \theta [2\epsilon_1(\lambda_1 - \epsilon_1)(\bar{\lambda}_1 - \epsilon_1) + s(\lambda_1 + \bar{\lambda}_1 - 2\epsilon_1)] = 0$$

It coincides with the pencil eq.(49) as can be seen by setting $\alpha = \cot \theta$. It is shown in Fig.[5]. Again, we stress that a specific circle of the pencil is specified by the direction in the (H_1, H_2) plane through which we reach the critical point. This is a typical blowup of a singularity.

As we see on Fig.[6], if we consider a generic torus close to the pinched torus containing the unstable point $P_1(\uparrow)$, the corresponding exact real slice in the λ_1 plane comprises a large circle and a segment very close to the line $\lambda_1 + \bar{\lambda}_1 - \epsilon_1 = 0$. This segment is absent from what we obtained from the quadratic normal form, which give us only the arc of circle belonging to the pencil.

To understand this, we first emphasize that replacing the moment map by its quadratic normal form has a dramatic effect on the real slice corresponding to the pinched torus: instead of the segment joining E and \bar{E} in the λ_1 plane, only the two end-points E and \bar{E} survive after making this quadratic approximation. Indeed, in the immediate vicinity of the critical point, the pinched torus has the shape of two cones that meet precisely at the critical point. One of these cones is

associated to the unstable small perturbations, namely those which are exponentially amplified, whereas the other cone corresponds to perturbations which are exponentially attenuated. Taking into account the reality conditions, we can parametrize as follows:

$$C_1 = A_1, \quad B_1 = \bar{A}_2, \quad C_2 = A_2, \quad B_2 = \bar{A}_1$$

The action variables are:

$$B_1 C_1 = A_1 \bar{A}_2, \quad B_2 C_2 = \bar{A}_1 A_2$$

When we are sitting right on the pinched torus, these two action variables should vanish. We have two ways to do it corresponding to the stable and unstable cones:

$$A_1 = 0, \quad A_2 \neq 0, \quad \text{or} \quad A_1 \neq 0, \quad A_2 = 0$$

Inserting into eq.(50) we see that they correspond to $\lambda_1 = E_1$ and $\lambda_1 = E_2$ respectively. Hence the variable λ_1 remains trapped at these points in this approximation.

Now, consider a solution of the equations of motion, and suppose we pick an initial condition close to the critical point $P_1(\uparrow)$, but not exactly on the pinched torus. Let us further assume that this initial condition is much closer to the stable cone than to the unstable one. The point representing the system in configuration space will first move towards $P_1(\uparrow)$ along the stable cone, but after a finite time, while remaining close to $P_1(\uparrow)$, it will be ejected away from it along the unstable cone. This part of the movement takes place in the vicinity of $P_1(\uparrow)$ and is well captured by the quadratic normal form. It corresponds to the arc of circle that connects the complex root E_s associated to the stable cone to its complex conjugate E_u associated to the unstable cone. This part of the trajectory has no counterpart when we are exactly on the pinched torus.

After this, the point representing the system goes far away from $P_1(\uparrow)$ along the unstable cone, and the quadratic normal form is no longer valid. But of course, the two cones are connected and any initial condition located on the unstable cone gives rise to a trajectory which reaches eventually the stable cone in a finite time. This is manifested by the part of the trajectory in the λ_1 plane which remains close to the finite segment of the line eq.(48) that connects E_u to E_s . This part is fully non-perturbative, in the sense that it cannot be captured by the quadratic normal form, but it is very well approximated by the large motion along the pinched torus.

In a sense the separated variable λ_1 and the normal coordinate C_i play complementary role and are each well adapted to describe a different part of the trajectory. The need to glue these two qualitatively different parts on a trajectory close to a pinched torus is an important feature which played a crucial role in our semi-classical treatment of the model [18].

4 Critical torii associated to equilibrium points for general n .

In this section, we study the level set of a critical point where the rank of the moment map is zero. In Fig.[1] these are the pre-images of the green (stable) and red (unstable) points. Hence, we

consider the critical points of the moment map (rank zero).

$$b = \bar{b} = 0, \quad s_j^z = se_j, \quad s_j^\pm = 0, \quad e_j = \pm 1$$

We know that they correspond to maximally degenerate spectral curves where:

$$Q_{2n+2}(\lambda) = 4 \prod_{l=1}^{n+1} (\lambda - E_l)^2 \quad (51)$$

From eq.(33) we also know that the zeroes of $Q_{2n+2}(\lambda)$ are the roots of the classical Bethe equation:

$$2E + \sum_{j=1}^n \frac{se_j}{E - \epsilon_j} = 0 \quad (52)$$

Notice that we have the identities:

$$2 \frac{\prod_k (\epsilon_j - E_k)}{\prod_{k \neq j} (\epsilon_j - \epsilon_k)} = se_j, \quad \sum_l E_l = \sigma_1(\epsilon)$$

The variables μ_i are given by

$$\mu_i = \pm 2 \frac{\prod_l (\lambda_i - E_l)}{\prod_j (\lambda_i - \epsilon_j)}$$

As we have seen in the one spin case, the choice of sign here plays a crucial role in the description of the various strata of the level set.

We will study the strata of the level set by constructing the solutions of the equations of motion with generic initial conditions on the level set. The equations of motion eq.(20) become

$$\dot{\lambda}_i = \pm 2i \frac{\prod_l (\lambda - E_l)}{\prod_{j \neq i} (\lambda_i - \lambda_j)}$$

We wish to solve these equations with the proper choice of signs and initial conditions so that the spins variables are real.

We first reconstruct the spin variables. The s_j^+ are given by:

$$s_j^+(t) = \frac{2\bar{b}(t)}{\prod_{k \neq j} (\epsilon_j - \epsilon_k)} \mathcal{P}(\epsilon_j, t) \quad (53)$$

where we have introduced the polynomial:

$$\mathcal{P}(\lambda, t) = \prod_j (\lambda - \lambda_j(t))$$

To reconstruct s_j^z , we have to build the polynomial $P_{n+1}(\lambda)$. From eqs.(22,51), we have:

$$P_{n+1}(\lambda_i) = \pm\sqrt{Q_{2n+2}(\lambda_i)} = \pm 2 \prod_l (\lambda_i - E_l), \quad P_{n+1}(\lambda) = 2(\lambda^{n+1} - \sigma_1(\epsilon)\lambda^n + \dots)$$

The choice of signs here is crucial. It is the same signs which appear in the equations of motion.

If we take the + sign for all i , then obviously $P_{n+1}(\lambda) = 2 \prod_l (\lambda - E_l)$, and taking the residue at $\lambda = \epsilon_j$ in $P_{n+1}(\lambda) / \prod_i (\lambda - \epsilon_i)$, we find $s_j^z = s\epsilon_j$. This is the static solution corresponding to the critical point.

To go beyond this trivial solution, we divide the λ_i into three sets $\lambda_i^+ \in \mathcal{E}^+$, $\lambda_i^0 \in \mathcal{E}^0$ and $\lambda_i^- \in \mathcal{E}^-$ depending on the sign in this formula. In particular \mathcal{E}^0 is the set of λ_i frozen at some E_l . The equations of motion become:

$$\partial_t \lambda_i^- = -2i \frac{\prod_l' (\lambda_i^- - E_l)}{\prod_j' (\lambda_i^- - \lambda_j)}, \quad \partial_t \lambda_i^+ = 2i \frac{\prod_l' (\lambda_i^+ - E_l)}{\prod_j' (\lambda_i^+ - \lambda_j)} \quad (54)$$

where the prime means that elements in the set \mathcal{E}^0 are excluded because they cancel between numerator and denominator. Therefore, for each $E_l \notin \mathcal{E}^0$ we can write:

$$\sum_{\lambda_i^-} \frac{\dot{\lambda}_i^-}{\lambda_i^- - E_l} - \sum_{\lambda_i^+} \frac{\dot{\lambda}_i^+}{\lambda_i^+ - E_l} = -2i \int_{C_\infty} \frac{dz}{2i\pi} \frac{\prod_{k \neq l}' (z - E_k)}{\prod_j' (z - \lambda_j)} = -2i(\Sigma_1' - \sigma_1'(E) + E_l)$$

where C_∞ is a big circle at infinity surrounding all the λ_j and we have defined $\Sigma_1' = \sum_j' \lambda_j$, $\sigma_1'(E) = \sum_k' E_k$. Hence:

$$\log \frac{\mathcal{P}_-(E_l)}{\mathcal{P}_+(E_l)} = -2iE_l t - 2i \int^t dt (\Sigma_1' - \sigma_1'(E))$$

where we have defined the polynomials:

$$\mathcal{P}_\pm(\lambda) = \prod_{\lambda_i^{(\pm)} \in \mathcal{E}^{(\pm)}} (\lambda - \lambda_i^{(\pm)}), \quad \mathcal{P}_0(\lambda) = \prod_{\lambda_i^0 \in \mathcal{E}^0} (\lambda - \lambda_i^0)$$

Remembering that

$$\dot{\bar{b}} = -2i\bar{b}(\Sigma_1' - \sigma_1'(E) - \omega/2)$$

we arrive at:

$$\mathcal{P}_-(E_l) = \bar{b}(t) X_l \mathcal{P}_+(E_l), \quad X_l = X_l(0) e^{-i(2E_l + \omega)t}, \quad E_l \notin \mathcal{E}^0 \quad (55)$$

Denoting n_\pm, n_0 the number of elements in $\mathcal{E}^{(\pm)}, \mathcal{E}^0$ respectively, we get a set of $n - n_0 + 1$ linear equations for the $n_+ + n_- + 1 = n - n_0 + 1$ unknown coefficients of the polynomials $\mathcal{P}_-(\lambda)$

and $\bar{b}(t)\mathcal{P}_+(\lambda)$. As discussed in subsection 2.3, we expect that freezing n_0 separated variables λ_j yields a stratum of dimension $n - n_0 + 1$ on the pre-image of the moment map corresponding to the degenerate spectral curve.

Simple examination of the quadratic normal form of section 9 shows that the complex numbers $2E_l + \omega$ are the eigenfrequencies for the linearized equations of motion in the vicinity of the critical point. Eq. (55) can therefore be interpreted as a non linear superposition of normal modes yielding a global motion along the critical torus.

The next step is to build the polynomial $P_{n+1}(\lambda)$, using the fact that $P_{n+1}(\lambda_i) = \pm 2 \prod_l (\lambda_i - E_l)$:

$$P_{n+1}(\lambda) = 2 \prod_l (\lambda - E_l) - 4 \sum_{\lambda_i^-} \prod_{E_l \notin \mathcal{E}^0} (\lambda_i^- - E_l) \frac{\prod_{\lambda_l^- \neq \lambda_i^-} (\lambda - \lambda_l^-)}{\prod_{\lambda_l^- \neq \lambda_i^-} (\lambda_i^- - \lambda_l^-)} \frac{\mathcal{P}_+(\lambda) \mathcal{P}_0(\lambda)}{\mathcal{P}_+(\lambda_i^-)}$$

To derive this formula, we used the fact that the polynomials $P_{n+1}(\lambda)$ and $2 \prod_l (\lambda - E_l)$ have the same terms of degrees $n+1$ and n ; the last statement comes from the relation $\sum_j \epsilon_j = \sum_l E_l$ which is a direct consequence of the classical Bethe equation. Similarly, we can also write:

$$\begin{aligned} P_{n+1}(\lambda) &= -2 \prod_l (\lambda - E_l) + 4 \sum_{\lambda_i^+} \prod_{E_l \notin \mathcal{E}^0} (\lambda_i^+ - E_l) \frac{\prod_{\lambda_l^+ \neq \lambda_i^+} (\lambda - \lambda_l^+)}{\prod_{\lambda_l^+ \neq \lambda_i^+} (\lambda_i^+ - \lambda_l^+)} \frac{\mathcal{P}_-(\lambda) \mathcal{P}_0(\lambda)}{\mathcal{P}_-(\lambda_i^+)} \\ &\quad + 4(\lambda + \Sigma'_1 - \sigma'_1(E)) \mathcal{P}_+(\lambda) \mathcal{P}_-(\lambda) \mathcal{P}_0(\lambda) \end{aligned}$$

Note that the last term in the right hand side is necessary to adjust the terms of degree $n+1$ and n in λ between the two sides of the equation. Again, we used the relation $\sum_j \epsilon_j = \sum_l E_l$. These two expressions for $P_{n+1}(\lambda)$ motivate the following definitions of polynomials $\mathcal{S}_{\pm}(\lambda)$:

$$\begin{aligned} \mathcal{S}_+(\lambda) &= \sum_{\lambda_i^-} \prod_{E_l \notin \mathcal{E}^0} (\lambda_i^- - E_l) \frac{\prod_{\lambda_l^- \neq \lambda_i^-} (\lambda - \lambda_l^-)}{\mathcal{P}'_-(\lambda_i^-) \mathcal{P}_+(\lambda_i^-)} \\ \mathcal{S}_-(\lambda) &= \sum_{\lambda_i^+} \prod_{E_l \notin \mathcal{E}^0} (\lambda_i^+ - E_l) \frac{\prod_{\lambda_l^+ \neq \lambda_i^+} (\lambda - \lambda_l^+)}{\mathcal{P}'_+(\lambda_i^+) \mathcal{P}_-(\lambda_i^+)} + (\lambda + \Sigma'_1 - \sigma'_1(E)) \mathcal{P}_+(\lambda) \end{aligned}$$

so that we can write:

$$P_{n+1}(\lambda) = 2 \prod_l (\lambda - E_l) - 4 \mathcal{S}_+(\lambda) \mathcal{P}_+(\lambda) \mathcal{P}_0(\lambda) \quad (56)$$

$$P_{n+1}(\lambda) = -2 \prod_l (\lambda - E_l) + 4 \mathcal{S}_-(\lambda) \mathcal{P}_-(\lambda) \mathcal{P}_0(\lambda) \quad (57)$$

Note that $\mathcal{S}_+(\lambda)$ has degree $n_- - 1$ and $\mathcal{S}_-(\lambda)$ has degree $n_+ + 1$. Now, we have:

$$4 \prod_l (\lambda - E_l)^2 - P_{n+1}^2(\lambda) = 16 \mathcal{S}_-(\lambda) \mathcal{S}_+(\lambda) \mathcal{P}_0(\lambda) \mathcal{P}(\lambda) = 4 \bar{b} b \mathcal{P}(\lambda) \bar{\mathcal{P}}(\lambda)$$

where $\mathcal{P}(\lambda) = \prod_j (\lambda - \lambda_j) = \mathcal{P}_-(\lambda)\mathcal{P}_0(\lambda)\mathcal{P}_+(\lambda)$ and $\bar{\mathcal{P}}(\lambda) = \prod_j (\lambda - \bar{\lambda}_j)$ is the complex conjugate of $\mathcal{P}(\lambda)$, that is $\bar{\mathcal{P}}(\lambda) = \overline{\mathcal{P}(\bar{\lambda})}$. Therefore:

$$\bar{b}b \bar{\mathcal{P}}(\lambda) = 4 \mathcal{S}_-(\lambda)\mathcal{S}_+(\lambda)\mathcal{P}_0(\lambda) \quad (58)$$

So the zeroes $\bar{\lambda}_i$ of $\bar{\mathcal{P}}(\lambda)$ split into the zeroes $\bar{\lambda}_i^+$, $\bar{\lambda}_i^-$ and $\bar{\lambda}_i^0$ of $\mathcal{S}_+(\lambda)$, $\mathcal{S}_-(\lambda)$ and $\mathcal{P}_0(\lambda)$ respectively. A direct consequence of these definitions and of eqs. (56) and (57) is that:

$$P_{n+1}(\bar{\lambda}_i^+) = +2 \prod_l (\bar{\lambda}_i^+ - E_l) \quad (59)$$

$$P_{n+1}(\bar{\lambda}_i^-) = -2 \prod_l (\bar{\lambda}_i^- - E_l) \quad (60)$$

By the definition of the $\bar{\lambda}_i^0$'s, we see that the set \mathcal{E}^0 is self conjugate (see section 2.3) and that $\mathcal{P}_0(\lambda) = \bar{\mathcal{P}}_0(\lambda)$. The above definition of $\mathcal{S}_-(\lambda)$ shows that the coefficient of its term of highest degree is equal to one (this is *not* the case for $\mathcal{S}_+(\lambda)$). Because of this:

$$\mathcal{S}_-(\lambda) = \bar{\mathcal{P}}_-(\lambda) \quad (61)$$

Combining this with eq. (58) we get also:

$$\mathcal{S}_+(\lambda) = \frac{1}{4} \bar{b}b \bar{\mathcal{P}}_+(\lambda) \quad (62)$$

Comparing the terms of highest degrees in $\mathcal{S}_+(\lambda)$ and $\bar{\mathcal{P}}_+(\lambda)$ gives:

$$\bar{b}b = 4 \sum_{\lambda_i^-} \frac{\prod_{E_l \notin \mathcal{E}^0} (\lambda_i^- - E_l)}{\mathcal{P}'_-(\lambda_i^-)\mathcal{P}_+(\lambda_i^-)} \quad (63)$$

It is expressed only in terms of λ_i^- 's. So, if $n_- = 0$, we recover the fact already mentioned that $\bar{b}b = 0$ and the system remains at the critical point.

At this stage, we are ready to enforce the reality condition. As discussed in subsection 2.2, the real slice is obtained by imposing that the set $\{\bar{\lambda}_i\}$ be the same as the set $\{\lambda_i^*\}$, where in the rest of this section we denote by z^* the complex conjugate of z . Equivalently:

$$\bar{\mathcal{P}}(\lambda^*) = \mathcal{P}(\lambda)^*$$

for any λ . From the discussion in subsection 2.3, we know that the frozen variables λ_i^0 appear in complex conjugate pairs so that $\mathcal{P}_0(\lambda^*) = \mathcal{P}_0(\lambda)^*$. We also know that $\mathcal{P}_0(\lambda) = \bar{\mathcal{P}}_0(\lambda)$ so that $\bar{\mathcal{P}}_0(\lambda^*) = \mathcal{P}_0(\lambda)^*$. The above reality condition becomes then:

$$\bar{\mathcal{P}}_-(\lambda^*)\bar{\mathcal{P}}_+(\lambda^*) = \mathcal{P}_-(\lambda)^*\mathcal{P}_+(\lambda)^*$$

It is clearly sufficient to impose simultaneously:

$$\bar{\mathcal{P}}_-(\lambda^*) = \mathcal{P}_-(\lambda)^*, \quad \bar{\mathcal{P}}_+(\lambda^*) = \mathcal{P}_+(\lambda)^* \quad (64)$$

But we now claim that this condition is also necessary. This comes from the fact already noted that the sign of $P_{n+1}(\lambda)/\prod_l(\lambda - E_l)$ is positive for $\lambda = \lambda_i^+$ or $\lambda = \bar{\lambda}_i^+$ and negative for $\lambda = \lambda_i^-$ or $\lambda = \bar{\lambda}_i^-$. So the roots $\bar{\lambda}_i^+$ have to be complex conjugates of λ_i^+ and likewise, the roots $\bar{\lambda}_i^-$ have to be complex conjugates of λ_i^- . An interesting and useful consequence of this is that we must have $\deg \mathcal{P}_\pm = \deg \mathcal{S}_\pm = \deg \bar{\mathcal{P}}_\pm$, which requires $n_+ = n_- - 1$. Since $n_+ + n_0 + n_- = n$ we find:

$$n_+ = \frac{1}{2}(n - 1 - n_0), \quad n_- = \frac{1}{2}(n + 1 - n_0)$$

Because the coefficients of highest degrees of $\mathcal{P}_-(\lambda)$ and $\mathcal{P}_+(\lambda)$ are set equal to one, the above constraints (64) are equivalent to (assuming of course that $\bar{\mathcal{P}}_+(\lambda)$ and $\bar{\mathcal{P}}_-(\lambda)$ are mutually prime and similarly for $\mathcal{P}_+(\lambda)$ and $\mathcal{P}_-(\lambda)$).

$$\frac{\bar{\mathcal{P}}_-(\lambda^*)}{\bar{\mathcal{P}}_+(\lambda^*)} = \left(\frac{\mathcal{P}_-(\lambda)}{\mathcal{P}_+(\lambda)} \right)^*$$

We also note that we should add the constraint $\bar{b} = b^*$. This plus the fact that these two polynomials involve a total of $n_+ + n_-$ unknown coefficients, shows that it is necessary and sufficient to enforce the following conditions for the $n + 1 - n_0 = n_+ + n_- + 1$ roots E_l which don't belong to \mathcal{E}^0 :

$$\frac{\bar{\mathcal{P}}_-(E_l^*)}{\bar{b}\bar{\mathcal{P}}_+(E_l^*)} = \left(\frac{\mathcal{P}_-(E_l)}{\bar{b}\mathcal{P}_+(E_l)} \right)^* \quad (65)$$

As we have seen, the general solution of the Hamiltonian evolution on the critical torus, eq. (55) implies:

$$\frac{\mathcal{P}_-(E_l)}{\bar{b}\mathcal{P}_+(E_l)} = X_l \quad (66)$$

To evaluate the left-hand side of the conditions (65), we set $\lambda = E_l$ in eqs.(56, 57), which gives:

$$P_{n+1}(E_l) = -4\mathcal{S}_+(E_l)\mathcal{P}_+(E_l)\mathcal{P}_0(E_l), \quad P_{n+1}(E_l) = 4\mathcal{S}_-(E_l)\mathcal{P}_-(E_l)\mathcal{P}_0(E_l), \quad E_l \notin \mathcal{E}^0$$

and therefore:

$$\mathcal{S}_+(E_l)\mathcal{P}_+(E_l) = -\mathcal{S}_-(E_l)\mathcal{P}_-(E_l) \quad (67)$$

Since $\mathcal{P}_+(E_l) \neq 0$, and remembering eq.(55) this implies:

$$\frac{\mathcal{S}_-(E_l)}{\mathcal{S}_+(E_l)} = -\frac{1}{\bar{b}X_l}$$

But using eqs. (61) and (62), we get:

$$\frac{\bar{\mathcal{P}}_-(E_l^*)}{b\bar{\mathcal{P}}_+(E_l^*)} = -\frac{1}{4X_{\bar{l}}} \quad (68)$$

where we define the index \bar{l} to be such that $E_{\bar{l}} = E_l^*$. Given eqs. (66) and (68), the reality conditions (65) and the condition $\bar{b} = b^*$ are satisfied if and only if:

$$X_l^* X_{\bar{l}} = -\frac{1}{4} \quad (69)$$

Let us check that the above conditions also imply the fact that s_j^z is real for any j . For this, we have to satisfy the relation $P_{n+1}(\lambda^*) = P_{n+1}(\lambda)^*$. But, as we have just seen, conditions (69) imply that $\bar{\lambda}_i^{(\pm)} = (\lambda_i^{(\pm)})^*$. From this, combined with eqs. (59), (60) and the fact that the polynomial $\prod_i(\lambda - E_i)$ has real coefficients we see that:

$$P_{n+1}((\lambda_i^{(\pm)})^*) = P_{n+1}(\lambda_i^{(\pm)})^*$$

But since:

$$P_{n+1}((\lambda_i^0)^*) = P_{n+1}(\lambda_i^0)^* = 0$$

we get:

$$P_{n+1}(\lambda_i^*) = P_{n+1}(\lambda_i)^*$$

for all the n separated variables. And because $P_{n+1}(\lambda) = 2\lambda^{n+1} - 2\sigma_1(\epsilon)\lambda^n + \dots$, these n relations are sufficient to impose the fact that P_{n+1} has real coefficients.

Together with the solution (55) of the Hamiltonian evolution, the explicit form eq. (69) of the reality conditions characterize completely a class of solitons, which have been first constructed by Yuzbashyan [12], and called by him *normal solitons*. Applications will be given in sections 6 and 7 for systems with two and three spins. As expected, time disappears from these conditions so that they reduce to constraints on the integration constants:

$$X_l(0)^* X_{\bar{l}}(0) = -\frac{1}{4}$$

This characterizes a stratum of dimension $n - n_0 + 1$ on the real slice.

5 Case of n double zeroes.

Let us consider now critical values of the moment map whose pre-image contains configurations where the moment map has rank one. These are the points on the green and red lines in Fig.[1]. In this case, the spectral polynomial $Q_{2n+2}(\lambda)$ can be written as:

$$Q_{2n+2}(\lambda) = 4 p_2(\lambda) \prod_{i=1}^n (\lambda - E_i)^2, \quad p_2(\lambda) = \lambda^2 + b_1\lambda + b_0$$

We have seen that $p_2(\lambda)$ is positive for real λ . Hence

$$\Delta = b_1^2 - 4b_0 < 0$$

If n_r is the number of *real* zeroes, we must have $n = n_r + 2m$ because the complex E_i must come in complex conjugated pairs. As was explained in subsection 2.3, we must satisfy the relations:

$$b_1 = 2(\sigma_1(E) - \sigma_1(\epsilon)) \quad (70)$$

$$2\sigma_1(E) = 2\sigma_1(\epsilon) - \sum_j \frac{\alpha_j s}{\sqrt{p_2(\epsilon_j)}}$$

and

$$b_1 + \sum_j \frac{\alpha_j s}{\sqrt{p_2(\epsilon_j)}} = 0 \quad (71)$$

This has the same form as eq. (31) and plays the role of a compatibility relation between the *real* parameters b_1, b_0 . We get therefore a one parameter family of such spectral curves. As we have seen before, in the case of one spin, this family corresponds to the boundary of the image of the moment map in the (H_1, H_2) plane.

We set now:

$$\lambda = -\frac{b_1}{2} + \frac{\sqrt{|\Delta|}}{4}(\Lambda - \Lambda^{-1})$$

so that $p_2(\lambda)$ becomes a perfect square:

$$p_2(\lambda) = \frac{|\Delta|}{16}(\Lambda + \Lambda^{-1})^2$$

and:

$$Q_{2n+2}(\lambda) = 4 \left(\frac{\sqrt{|\Delta|}}{4} \right)^{2n+2} (\Lambda + \Lambda^{-1})^2 \prod_{i=1}^n (\Lambda - \Lambda^{-1} - 2A_i)^2$$

where:

$$A_i = \frac{b_1 + 2E_i}{\sqrt{|\Delta|}}$$

so that:

$$\sqrt{Q_{2n+2}(\lambda)} = 2 \left(\frac{\sqrt{|\Delta|}}{4} \right)^{n+1} (\Lambda + \Lambda^{-1}) \prod_{i=1}^n (\Lambda - \Lambda^{-1} - 2A_i) \equiv Q(\Lambda)$$

The sign of the square root is changed by the transformation $\Lambda \rightarrow -\Lambda^{-1}$. This transformation leaves λ invariant and corresponds therefore to the hyperelliptic involution on the spectral curve, which has been uniformized in the complex plane Λ .

The points $(\lambda_k, \pm\mu_k)$ correspond to the points $(\Lambda_k, Q(\Lambda_k))$ and $(-\Lambda_k^{-1}, Q(-\Lambda_k^{-1}) = -Q(\Lambda_k))$ in the complex Λ plane. Among these $2n$ points only n of them correspond to poles of the eigenvector. We denote them by Λ_k and the other ones are their image by the hyperelliptic involution $\Lambda_k^\eta = -\Lambda_k^{-1}$. As we know, when we have a double *real* zero E_i , one of the λ_i 's is frozen at E_i . Some other variables λ_i 's can be frozen by complex conjugate pairs on complex double roots. Let us denote by \mathcal{E}^0 the set of $n_0 \geq n_r$ values Λ_i corresponding to the frozen roots. We have $n_0 - n_r$ even and as a result, $n - n_0$ is also even.

The equations of motion eq.(20) become:

$$\frac{\dot{\Lambda}_k}{\Lambda_k} = \frac{\sqrt{|\Delta|}}{2} \frac{\prod'_i (\Lambda_k - \Lambda_k^{-1} - 2A_i)}{\prod'_{l \neq k} (\Lambda_k - \Lambda_k^{-1} - \Lambda_l + \Lambda_l^{-1})}$$

where the $'$ means that the terms corresponding to frozen roots are excluded because they cancel between numerator and denominator. From this, we deduce:

$$\sum'_k \frac{d\Lambda_k}{\Lambda_k^2 - 2A_j\Lambda_k - 1} = i \frac{\sqrt{|\Delta|}}{2} dt, \quad \forall j \notin \mathcal{E}^0$$

Introducing the roots of the denominators:

$$B_j = A_j + \sqrt{A_j^2 + 1}, \quad B_j^\eta = -B_j^{-1} = A_j - \sqrt{A_j^2 + 1}$$

the solution of the equations of motion is:

$$\frac{\prod'_k (\Lambda_k - B_j)}{\prod'_k (\Lambda_k - B_j^\eta)} = X_j, \quad X_j = X_j(0) e^{i\sqrt{|\Delta|}\sqrt{A_j^2+1}t}, \quad j \notin \mathcal{E}^0$$

Note that the eigenfrequencies $\sqrt{|\Delta|}\sqrt{A_j^2+1} = 2\sqrt{p_2(E_j)}$ have a slightly more complicated relation to the double roots E_j than in the case of a spectral polynomial with $n+1$ double roots studied before.

We introduce now the polynomials:

$$\mathcal{P}_+(\Lambda) = \prod'_k (\Lambda - \Lambda_k), \quad \mathcal{P}_+^\eta(\Lambda) = \prod'_k (\Lambda - \Lambda_k^\eta)$$

satisfying the useful formulae:

$$\mathcal{P}_+(\Lambda^\eta) = (-\Lambda)^{-n+n_0} \prod'_k \Lambda_k \mathcal{P}_+^\eta(\Lambda), \quad \mathcal{P}_+^\eta(\Lambda^\eta) = (\Lambda)^{-n+n_0} \prod'_k (\Lambda_k)^{-1} \mathcal{P}_+(\Lambda) \quad (72)$$

With these notations, the solution of the equation of motion becomes:

$$\mathcal{P}_+(B_j) = X_j \mathcal{P}_+(B_j^\eta) = X_j B_j^{-n+n_0} \prod'_k \Lambda_k \mathcal{P}_+^\eta(B_j) \quad (73)$$

These are $n - n_0$ equations for the normalised degree $n - n_0$ polynomial $\mathcal{P}_+(\Lambda)$ which is therefore completely determined. Note that unlike the case of a spectral polynomial with $n + 1$ double roots, we have access only to the evolution of separated variables (the variables b, \bar{b} do not appear in these formulae). In other words, this gives the dynamics of the reduced system, and the collective motion associated to the global $U(1)$ action has to be determined separately.

The next step is to find the polynomial $P_{n+1}(\lambda)$, which we express in the variable Λ . To simplify the notation, $P_{n+1}(\lambda(\Lambda))$ is a rational fraction in Λ which will be abusively denoted by $P_{n+1}(\Lambda)$. Note that with this notation $\Lambda^{n+1}P_{n+1}(\Lambda)$ is a polynomial of degree $2(n + 1)$ in Λ . We have the constraints:

$$P_{n+1}(\Lambda_k) = P_{n+1}(\Lambda_k^\eta) = Q(\Lambda_k) = -Q(\Lambda_k^\eta)$$

By analogy to eqs. (56), (57), we can write:

$$\Lambda^{n+1}P_{n+1}(\Lambda) = \Lambda^{n+1}Q(\Lambda) - 2\mathcal{S}_+(\Lambda)\mathcal{P}_+(\Lambda)\mathcal{P}_0(\Lambda)\mathcal{P}_0^\eta(\Lambda) \quad (74)$$

$$\Lambda^{n+1}P_{n+1}(\Lambda) = -\Lambda^{n+1}Q(\Lambda) + 2\mathcal{S}_-(\Lambda)\mathcal{P}_+^\eta(\Lambda)\mathcal{P}_0(\Lambda)\mathcal{P}_0^\eta(\Lambda) \quad (75)$$

The polynomials $\mathcal{P}_0(\Lambda)\mathcal{P}_0^\eta(\Lambda)$ are introduced because both $P_{n+1}(\Lambda)$ and $Q(\Lambda)$ vanish at those points. The coefficients of degree $2n + 2$ of $\Lambda^{n+1}P_{n+1}(\Lambda)$ and $\Lambda^{n+1}Q(\Lambda)$ are identical, and the same is true for the coefficients of degree $2n + 1$, because of the relation (70). This leads to:

$$\deg \mathcal{S}_+ = n - n_0, \quad \deg \mathcal{S}_- = n - n_0 + 2$$

These two polynomials are determined by the $n - n_0$ conditions:

$$\mathcal{S}_+(\Lambda_k^\eta) = -\frac{(\Lambda_k^\eta)^{n+1}Q(\Lambda_k)}{\mathcal{P}_+(\Lambda_k^\eta)\mathcal{P}_0(\Lambda_k^\eta)\mathcal{P}_0^\eta(\Lambda_k^\eta)}, \quad \mathcal{S}_-(\Lambda_k) = \frac{(\Lambda_k)^{n+1}Q(\Lambda_k)}{\mathcal{P}_+^\eta(\Lambda_k)\mathcal{P}_0(\Lambda_k)\mathcal{P}_0^\eta(\Lambda_k)}$$

and additional conditions at infinity. For example:

$$\mathcal{S}_-(\Lambda) = 2 \left(\frac{\sqrt{|\Delta|}}{4} \right)^{n+1} \Lambda^{n-n_0+2} + \dots$$

From $P_{n+1}(\Lambda) = P_{n+1}(\Lambda^\eta)$, and $Q(\Lambda) = -Q(\Lambda^\eta)$, we get:

$$\mathcal{S}_-(\Lambda) = \prod_k' \Lambda_k \Lambda^{n-n_0+2} \mathcal{S}_+(\Lambda^\eta) \quad (76)$$

Note that the quantity $\prod_k' \Lambda_k$ is given by the constant term in the polynomial $\mathcal{P}_+(\Lambda)$, which is reconstructed from the relations (73). Eq. (76) implies that $\mathcal{S}_-(\Lambda) \simeq \Lambda^2$ when $\Lambda \rightarrow 0$. Furthermore, the known coefficient of highest degree in $\mathcal{S}_-(\Lambda)$ determines the coefficient of lowest degree in $\mathcal{S}_+(\Lambda)$. The $n - n_0$ values of $\mathcal{S}_+(\Lambda_k^\eta)$ are then sufficient to reconstruct the polynomial $\mathcal{S}_+(\Lambda)$ because its degree is $n - n_0$.

Proceeding as before, we have:

$$\Lambda^{2n+2}(Q^2(\Lambda) - P_{n+1}^2(\Lambda)) = 4 \mathcal{S}_-(\Lambda)\mathcal{S}_+(\Lambda)\mathcal{P}(\Lambda)\mathcal{P}_0(\Lambda)\mathcal{P}_0^\eta(\Lambda) = 4 \left(\frac{\sqrt{|\Delta|}}{4} \right)^{2n} \bar{b}b \Lambda^2 \mathcal{P}(\Lambda)\bar{\mathcal{P}}(\Lambda)$$

where:

$$\mathcal{P}(\Lambda) = \mathcal{P}_+(\Lambda)\mathcal{P}_+^\eta(\Lambda)\mathcal{P}_0(\Lambda)\mathcal{P}_0^\eta(\Lambda), \quad \bar{\mathcal{P}}(\Lambda) = \bar{\mathcal{P}}_+(\Lambda)\bar{\mathcal{P}}_+^\eta(\Lambda)\bar{\mathcal{P}}_0(\Lambda)\bar{\mathcal{P}}_0^\eta(\Lambda)$$

Therefore:

$$\left(\frac{\sqrt{|\Delta|}}{4} \right)^{2n} \bar{b}b \Lambda^2 \bar{\mathcal{P}}(\Lambda) = \mathcal{S}_-(\Lambda)\mathcal{S}_+(\Lambda)\mathcal{P}_0(\Lambda)\mathcal{P}_0^\eta(\Lambda)$$

So we conclude that the frozen zeroes of $\bar{\mathcal{P}}(\Lambda)$ are the same as those of $\mathcal{P}(\Lambda)$, that is:

$$\bar{\mathcal{P}}_0(\Lambda)\bar{\mathcal{P}}_0^\eta(\Lambda) = \mathcal{P}_0(\Lambda)\mathcal{P}_0^\eta(\Lambda)$$

We have then:

$$\left(\frac{\sqrt{|\Delta|}}{4} \right)^{2n} \bar{b}b \Lambda^2 \bar{\mathcal{P}}_+(\Lambda)\bar{\mathcal{P}}_+^\eta(\Lambda) = \mathcal{S}_-(\Lambda)\mathcal{S}_+(\Lambda) \quad (77)$$

Hence, the non frozen zeroes of $\bar{\mathcal{P}}(\Lambda)$ split into the zeroes $\bar{\Lambda}_k$ of $\mathcal{S}_+(\Lambda)$ and $\bar{\Lambda}_k^\eta$ of $\mathcal{S}_-(\Lambda)$ and these two sets of zeroes are related by the hyperelliptic involution due to eq.(76). Notice that by eqs. (74), (75), we have:

$$P_{n+1}(\bar{\Lambda}_k) = +Q(\bar{\Lambda}_k), \quad P_{n+1}(\bar{\Lambda}_k^\eta) = -Q(\bar{\Lambda}_k^\eta)$$

which are indeed compatible. On the real slice, this will imply that $\bar{\Lambda}_k$ is the complex conjugate of Λ_k . Because $\mathcal{S}_-(\Lambda)$ is equal to Λ^2 times a polynomial of degree $n - n_0$ whose coefficient of highest degree is known, we get:

$$\mathcal{S}_-(\Lambda) = 2 \left(\frac{\sqrt{|\Delta|}}{4} \right)^{n+1} \Lambda^2 \bar{\mathcal{P}}_+^\eta(\Lambda) \quad (78)$$

Substituting this equality in eq.(77), we find:

$$\mathcal{S}_+(\Lambda) = \frac{1}{2} \left(\frac{\sqrt{|\Delta|}}{4} \right)^{n-1} \bar{b}b \bar{\mathcal{P}}_+(\Lambda), \quad (79)$$

Inserting into eq.(76) we find the compatibility relation:

$$\bar{b}b = \frac{|\Delta|}{4} \frac{1}{\prod'_k \Lambda_k \prod'_k \bar{\Lambda}_k}$$

where we have used the fact that $n - n_0$ is even so that $(-1)^{n-n_0} = 1$.

Let us now turn to the real slice. Reasoning in the same way as in section 4, it is necessary and sufficient to impose the $n - n_0$ conditions:

$$\frac{\mathcal{P}_+(B_l^*)}{\mathcal{P}_+(B_l^{\eta*})} = \left(\frac{\bar{\mathcal{P}}_+(B_l)}{\bar{\mathcal{P}}_+(B_l^\eta)} \right)^*$$

which are equivalent to (recall that $\mathcal{P}_+(0) = \prod' \Lambda_k$):

$$\frac{\mathcal{P}_+(B_l^*)}{\mathcal{P}_+(0)\mathcal{P}_\eta^+(B_l^*)} = \left(\frac{\bar{\mathcal{P}}_+(B_l)}{\bar{\mathcal{P}}_+(0)\bar{\mathcal{P}}_\eta^+(B_l)} \right)^* \quad (80)$$

From eq. (73), we have:

$$\frac{\mathcal{P}_+(B_l^*)}{\mathcal{P}_+(0)\mathcal{P}_\eta^+(B_l^*)} = X_{\bar{l}}(B_l^*)^{-n+n_0} \quad (81)$$

To express the right-hand side in eq. (80), we write eqs.(74), (75) for $\Lambda = B_l$, where $l \notin \mathcal{E}^0$:

$$\begin{aligned} B_l^{n+1}P_{n+1}(B_l) &= -2\mathcal{S}_+(B_l)\mathcal{P}_+(B_l)\mathcal{P}_0(B_l)\mathcal{P}_0^\eta(B_l) \\ B_l^{n+1}P_{n+1}(B_l) &= 2\mathcal{S}_-(B_l)\mathcal{P}_+^\eta(B_l)\mathcal{P}_0(B_l)\mathcal{P}_0^\eta(B_l) \end{aligned}$$

and therefore:

$$\mathcal{S}_+(B_l)\mathcal{P}_+(B_l) = -\mathcal{S}_-(B_l)\mathcal{P}_+^\eta(B_l), \quad l \notin \mathcal{E}^0 \quad (82)$$

Remembering eq.(73) this implies:

$$\mathcal{S}_-(B_l) = (-1)^{n-n_0+1} B_l^{-n+n_0} X_l \prod'_k \Lambda_k \mathcal{S}_+(B_l)$$

Using eqs.(78), (79), we arrive at:

$$\frac{\bar{\mathcal{P}}_+(B_l)}{\bar{\mathcal{P}}_+(0)\bar{\mathcal{P}}_\eta^+(B_l)} = -\frac{B_l^{n-n_0+2}}{X_l} \quad (83)$$

Taking into account eqs. (81) and (83), the reality conditions (80) become:

$$X_l^* X_{\bar{l}} = -(B_l^*)^{2n-2n_0+2} \quad (84)$$

Time disappears from these conditions which reduce to constraints on the integration constants:

$$X_l(0)^* X_{\bar{l}}(0) = -(B_l^*)^{2n-2n_0+2}, \quad l \notin \mathcal{E}^0$$

Together with the solution (73) of the Hamiltonian flow, these equations characterize completely any stratum of dimension $n - n_0 + 1$ on the real slice where n_0 separated variables are frozen on the double roots of the spectral polynomial. They correspond to the *anomalous solitons* in Yuzbashyan's terminology [12].

6 The two-spins model.

We now give some details on the two spins model. Let us first write explicitly the Hamiltonians:

$$\begin{aligned} H_1 &= 2\epsilon_1 s_1^z + b s_1^+ + \bar{b} s_1^- + \frac{\vec{s}_1 \cdot \vec{s}_2}{\epsilon_1 - \epsilon_2} \\ H_2 &= 2\epsilon_2 s_2^z + b s_2^+ + \bar{b} s_2^- - \frac{\vec{s}_1 \cdot \vec{s}_2}{\epsilon_1 - \epsilon_2} \\ H_3 &= \bar{b} b + s_1^z + s_2^z \end{aligned}$$

where $\vec{s}_1 \cdot \vec{s}_2 = s_1^z s_2^z + \frac{1}{2}(s_1^- s_2^+ + s_1^+ s_2^-)$. The singular points are given by $b = \bar{b} = 0$, $s_1^\pm = s_2^\pm = 0$ so that we have four of them: $s_1^z = \pm s$, $s_2^z = \pm s$. The corresponding values $P = (H_1, H_2, H_3)$ are:

$$\begin{aligned} P_1(\uparrow, \uparrow) &= \left[\frac{s^2}{\epsilon_1 - \epsilon_2} + 2\epsilon_1 s, \quad 2\epsilon_2 s - \frac{s^2}{\epsilon_1 - \epsilon_2}, \quad 2s \right] \\ P_2(\uparrow, \downarrow) &= \left[2\epsilon_1 s - \frac{s^2}{\epsilon_1 - \epsilon_2}, \quad \frac{s^2}{\epsilon_1 - \epsilon_2} - 2\epsilon_2 s, \quad 0 \right] \\ P_3(\downarrow, \uparrow) &= \left[-2\epsilon_1 s - \frac{s^2}{\epsilon_1 - \epsilon_2}, \quad \frac{s^2}{\epsilon_1 - \epsilon_2} + 2\epsilon_2 s, \quad 0 \right] \\ P_4(\downarrow, \downarrow) &= \left[\frac{s^2}{\epsilon_1 - \epsilon_2} - 2\epsilon_1 s, \quad -2\epsilon_2 s - \frac{s^2}{\epsilon_1 - \epsilon_2}, \quad -2s \right] \end{aligned}$$

In order to determine the type of the singularities we write the classical Bethe equations:

$$a(E) = 2E + \frac{se_1}{E - \epsilon_1} + \frac{se_2}{E - \epsilon_2} = 0 \quad (85)$$

These are polynomial equations of degree 3. The type of the singularity is determined by the number of real roots of these equations. If we have three real roots we have a stable elliptic singularity and if we have one real root we have an unstable focus-focus singularity. We easily see that $P_4(\downarrow, \downarrow)$ is always stable. See [11] for a detailed discussion of the parameter space (ϵ_1, ϵ_2) .

6.1 Image of the moment map.

The spectral curve reads in this case:

$$\mu^2 = \frac{Q_6(\lambda)}{(\lambda - \epsilon_1)^2(\lambda - \epsilon_2)^2} = 4\lambda^2 + 4H_3 + \frac{2H_1}{\lambda - \epsilon_1} + \frac{2H_2}{\lambda - \epsilon_2} + \frac{s^2}{(\lambda - \epsilon_1)^2} + \frac{s^2}{(\lambda - \epsilon_2)^2} \quad (86)$$

The image of the moment map can be drawn from the degenerations of this curve. An example is shown in Fig.[1]. In this example the parameters (ϵ_1, ϵ_2) have been chosen such that the points $P_2(\uparrow, \downarrow)$, $P_4(\downarrow, \downarrow)$ are stable while the points $P_1(\uparrow, \uparrow)$ and $P_3(\downarrow, \uparrow)$ are unstable.

The spin variables are reconstructed from the separated variables (λ_i, μ_i) , $i = 1, 2$. In particular, we have:

$$s_1^z = 2 \frac{(\epsilon_1 - \lambda_1)(\epsilon_1 - \lambda_2)}{\epsilon_1 - \epsilon_2} (\lambda_1 + \lambda_2 - \epsilon_2) - \nu_1 \frac{\lambda_2 - \epsilon_1}{(\lambda_1 - \lambda_2)(\epsilon_1 - \epsilon_2)} - \nu_2 \frac{\lambda_1 - \epsilon_1}{(\lambda_2 - \lambda_1)(\epsilon_1 - \epsilon_2)} \quad (87)$$

$$s_2^z = 2 \frac{(\epsilon_2 - \lambda_1)(\epsilon_2 - \lambda_2)}{\epsilon_2 - \epsilon_1} (\lambda_1 + \lambda_2 - \epsilon_1) - \nu_1 \frac{\lambda_2 - \epsilon_2}{(\lambda_1 - \lambda_2)(\epsilon_2 - \epsilon_1)} - \nu_2 \frac{\lambda_1 - \epsilon_2}{(\lambda_2 - \lambda_1)(\epsilon_2 - \epsilon_1)} \quad (88)$$

where $\nu_i = (\lambda_i - \epsilon_1)(\lambda_i - \epsilon_2)\mu_i$.

6.2 Rank zero.

The critical points are the points where the rank of the moment map is zero. They correspond to the complete degeneracy of the spectral curve:

$$\mu^2 = a^2(\lambda)$$

where $a(\lambda)$ is given eq.(109). The pre-images of these points are reduced to a point, in the case of a stable critical point, or to a pinched torus in the case of an unstable critical point. In that case non trivial solutions of the equations of motion exist which we now study.

So, let

$$Q_6(\lambda) = 4(\lambda - E_0)^2(\lambda - E)^2(\lambda - \bar{E})^2 \quad (89)$$

where E_0, E, \bar{E} are the three roots of eq.(85). We assume that E_0 is real E is complex and \bar{E} is the complex conjugate of E . We have the following relations coming from eq.(85):

$$\begin{aligned} E_0 + E + \bar{E} &= \epsilon_1 + \epsilon_2 \\ E\bar{E} + E_0E + E_0\bar{E} &= \epsilon_1\epsilon_2 + \frac{s}{2}(e_1 + e_2) \\ E_0E\bar{E} &= \frac{s}{2}(e_1\epsilon_2 + e_2\epsilon_1) \end{aligned}$$

Since there is a double real zero, we must freeze one point of the divisor :

$$\lambda_2 = E_0, \quad \mu_2 = 0$$

then there remains only (λ_1, μ_1) with

$$\mu_1 = \pm 2 \frac{(\lambda_1 - E_0)(\lambda_1 - E)(\lambda_1 - \bar{E})}{(\lambda_1 - \epsilon_1)(\lambda_1 - \epsilon_2)}$$

then from eqs.(87), (88) we get immediately:

$$\begin{aligned} s_1^z &= -2 \frac{\epsilon_1 - E_0}{\epsilon_1 - \epsilon_2} \left((\lambda_1 + E_0 - \epsilon_2)(\lambda_1 - \epsilon_1) \mp (\lambda_1 - E)(\lambda_1 - \bar{E}) \right) \\ s_2^z &= -2 \frac{\epsilon_2 - E_0}{\epsilon_2 - \epsilon_1} \left((\lambda_1 + E_0 - \epsilon_1)(\lambda_1 - \epsilon_2) \mp (\lambda_1 - E)(\lambda_1 - \bar{E}) \right) \end{aligned}$$

The upper sign leads to the constant solution $s_i^z = se_i$ as we already know. So we choose the lower sign. Reality of s_i^z requires:

$$\lambda_1 + \bar{\lambda}_1 = E + \bar{E}$$

and we can write:

$$\begin{aligned} s_1^z &= -2 \frac{\epsilon_1 - E_0}{\epsilon_1 - \epsilon_2} \left(-2\lambda_1 \bar{\lambda}_1 + \epsilon_1(\epsilon_2 - E_0) + E\bar{E} \right) \\ s_2^z &= -2 \frac{\epsilon_2 - E_0}{\epsilon_2 - \epsilon_1} \left(-2\lambda_1 \bar{\lambda}_1 + \epsilon_2(\epsilon_1 - E_0) + E\bar{E} \right) \end{aligned}$$

The equation of motion becomes:

$$\frac{d\lambda_1}{dt} = 2i(\lambda_1 - E)(\lambda_1 - \bar{E})$$

This is exactly the same equation as eq.(41), whose solution is given by eq.(42). It reads:

$$\lambda_1 = \frac{E - \bar{E}X}{1 - X}, \quad X = X(0)e^{2i(E-\bar{E})t}, \quad X(0) \text{ real} < 0.$$

These solutions exist on the pre-images of the red and blue dots in Fig.[1].

6.3 Rank one.

The lines of rank one correspond to the following degeneracy of the spectral curve:

$$Q_6(\lambda) = 4(\lambda^2 + a_1\lambda + a_0)^2(\lambda^2 + b_1\lambda + b_0) \quad (90)$$

We have four coefficients and three conditions on $Q_6(\lambda)$. Hence we have a dimension one manifold of solutions. The coefficients b_j are completely determined and there is one constraint between (a_0, a_1) . Note that the case of rank 0 is obtained as a special case of rank 1, when the polynomial $\lambda^2 + b_1\lambda + b_0$ has a doubly degenerate root, which is necessarily real. Let us parametrize (a_0, a_1) in terms of (x, y) as follows:

$$a_0 = -\frac{\epsilon_1 y + \epsilon_2 x - 2\epsilon_1 \epsilon_2}{2}, \quad a_1 = \frac{y + x - 2\epsilon_2 - 2\epsilon_1}{2}$$

Imposing the vanishing of the coefficient of λ in eq.(86), we find:

$$b_1 = -(y + x)$$

Imposing that the coefficient of the double pole at $\lambda = \epsilon_2$ is s^2 we find:

$$b_0 = \frac{(\epsilon_2 y^3 + \epsilon_2 x y^2 - \epsilon_2^2 y^2 + s^2)}{y^2}$$

Imposing that the coefficient of the double pole at $\lambda = \epsilon_1$ is s^2 we find that the parameters x and y are tied together by the relation:

$$S_1 : \quad s^2(y^2 - x^2) + (\epsilon_1 - \epsilon_2)(x + y - \epsilon_1 - \epsilon_2)x^2 y^2 = 0 \quad (91)$$

This is nothing but eq.(71) when we set:

$$x = \frac{e_1 s}{\sqrt{p_2(\epsilon_1)}}, \quad y = \frac{e_2 s}{\sqrt{p_2(\epsilon_2)}}$$

Once the spectral curve is known, we can read the values of the Hamiltonians H_i by writing it in the form eq.(86). They read:

$$H_1 = -\frac{1}{2}x^3 - \frac{1}{2}yx^2 + \epsilon_1 x^2 + \frac{2s^2}{(\epsilon_1 - \epsilon_2)x}(y + 2\epsilon_1 - 2\epsilon_2) \quad (92)$$

$$H_2 = -\frac{1}{2}y^3 - \frac{1}{2}xy^2 + \epsilon_2 y^2 - \frac{2s^2}{(\epsilon_1 - \epsilon_2)y}(x - 2\epsilon_1 + 2\epsilon_2) \quad (93)$$

$$H_3 = -\frac{3}{4}(x + y - \epsilon_1 - \epsilon_2)^2 - \epsilon_2 x - \epsilon_1 y + \epsilon_1 \epsilon_2 + \frac{1}{4}(\epsilon_1 + \epsilon_2)^2 + \frac{s^2}{2x^2} + \frac{s^2}{2y^2} \quad (94)$$

Together with eq.(91) these are the parametric equations of the lines of rank one of the moment map.

As we have seen, the discriminant $b_1^2 - 4b_0b_2 \leq 0$. It is zero when we are at a critical point, in which case $\lambda^2 + b_1\lambda + b_0 = (\lambda - E_0)^2$ with E_0 real. But as soon as we leave the critical point it becomes strictly negative so that:

$$\lambda^2 + b_1\lambda + b_0 = (\lambda - E_0)(\lambda - \bar{E}_0)$$

with E_0 and \bar{E}_0 being complex conjugate. The difference between the green lines and the red lines in Fig.[1] comes from the sign of the other discriminant $a_1^2 - 4a_0$. This leads to two very different situations which we describe below.

First when $a_1^2 - 4a_0$ is *positive* the polynomial $\lambda^2 + a_1\lambda + a_0 = (\lambda - E_1)(\lambda - E_2)$ has two *real* roots, so that $Q_6(\lambda)$ has two double real roots. According to the general discussion we must freeze two separate variables on these roots, and hence λ_1 and λ_2 are completely frozen. This corresponds to a static solution of the reduced model and therefore to a Liouville torus reduced to a circle S^1 in the original model. This circle can be easily described. We can compute the components s_j^z of the spins by setting $(\lambda_1 = E_1, \mu_1 = 0)$, $(\lambda_2 = E_2, \mu_2 = 0)$ in eqs.(87), (88). We find:

$$s_1^z = 2 \frac{(\epsilon_1 - E_1)(\epsilon_1 - E_2)}{(\epsilon_1 - \epsilon_2)}(E_1 + E_2 - \epsilon_2) = \frac{1}{2}x(2\epsilon_1 - x - y) \quad (95)$$

$$s_2^z = 2 \frac{(\epsilon_2 - E_1)(\epsilon_2 - E_2)}{(\epsilon_2 - \epsilon_1)}(E_1 + E_2 - \epsilon_1) = \frac{1}{2}y(2\epsilon_2 - x - y) \quad (96)$$

The spins simply have a uniform rotation around the z -axis. The quantity $\bar{b}b$ is constant and can be calculated from $\bar{b}b = H_2 - s_1^z - s_2^z$. This is the situation that prevails when we move along a green line in Fig.[1].

The other situation occurs when $a_1^2 - 4a_0$ is *negative*. The polynomial $\lambda^2 + a_1\lambda + a_0 = (\lambda - E)(\lambda - \bar{E})$ has now two *complex* conjugated roots, so that $Q_6(\lambda)$ has pair of complex conjugated double roots. This is the situation when we move on a red line in Fig.[1] until the discriminant eventually vanishes. At this point the two roots (E, \bar{E}) become a double real root (so that $Q_6(\lambda)$ has a quadruple real root there). Beyond that point we have two real roots and the color of the line turns green.

The pre-image of a point on a rank one line can be conveniently understood in the vicinity of a critical point by using normal forms. Around a stable critical point, we have three elliptic normal modes. At the critical point the three action variables corresponding to these modes are equal to zero. When we leave the critical point on a rank one line, two action variables are kept equal to zero, and a third one becomes non zero. We get the three lines leaving the critical point from the three possible choices of the non zero action variable. The pre-image of a point on these lines is a circle.

Around an unstable point, we have one focus-focus mode and one elliptic mode. The neighborhood of the critical point on the two dimensional face on which it lies is obtained by the activation of the action variables of the focus-focus mode, keeping the action variables of the elliptic mode equal to zero. On the other hand, the rank one line leaving the critical point corresponds to the action variable associated to the elliptic mode becoming non zero while the two action variables associated to the focus-focus mode remain zero. In phase space, the pre-image associated to the elliptic mode is a circle, while the pre-image associated to the focus-focus modes is a pinched torus. Hence the pre-image of a point on the rank one line is the product of a circle and a pinched torus.

As long as $a_1^2 - 4a_0$ is *negative*, there exist non trivial solutions of the equations of motion. So, let us concentrate on that case:

$$Q_6(\lambda) = 4(\lambda - E)^2(\lambda - \bar{E})^2(\lambda - E_0)(\lambda - \bar{E}_0)$$

One simple solution in this case is to freeze the separated variables on the pair of complex conjugated double roots $(\lambda_1 = E, \mu_1 = 0)$, $(\lambda_2 = \bar{E}, \mu_2 = 0)$. This static solution corresponds precisely to a circle in the original model, and eqs.(95,96) are still valid in this case. This is the stratum $n = 2, n_0 = 2$ in the general theory.

But we know that there exists another stratum, $n = 2, n_0 = 0$, of dimension 3 in the original model and 2 in the reduced model, corresponding to big motions on the pinched torus mentioned above. To uniformize the spectral curve, we set as before:

$$\lambda = \frac{E_0 + \bar{E}_0}{2} + \frac{E_0 - \bar{E}_0}{4i}(\Lambda - \Lambda^{-1}) = -\frac{b_1}{2} + \frac{\sqrt{|\Delta|}}{4}(\Lambda - \Lambda^{-1}) \quad (97)$$

so that:

$$(\lambda - E)(\lambda - \bar{E}) = \frac{|\Delta|}{16} \frac{1}{\Lambda^2} (\Lambda^2 - A\Lambda - 1) (\Lambda^2 - \bar{A}\Lambda - 1)$$

where we have set:

$$A = \frac{b_1 + 2E}{\sqrt{|\Delta|}}, \quad \bar{A} = \frac{b_1 + 2\bar{E}}{\sqrt{|\Delta|}}$$

We introduce the coordinates (Λ_1, Λ_2) associated to (λ_1, λ_2) and the polynomial $\mathcal{P}_+(\Lambda) = (\Lambda - \Lambda_1)(\Lambda - \Lambda_2)$. The solution of the equations of motion is given by:

$$(\Lambda_1 - B_1)(\Lambda_2 - B_1) = X_1(t)(\Lambda_1 - B_1^\eta)(\Lambda_2 - B_1^\eta) \quad (98)$$

$$(\Lambda_1 - B_{\bar{1}})(\Lambda_2 - B_{\bar{1}}) = X_{\bar{1}}(t)(\Lambda_1 - B_{\bar{1}}^\eta)(\Lambda_2 - B_{\bar{1}}^\eta) \quad (99)$$

where:

$$B_1 = A + \sqrt{A^2 + 1}, \quad B_1^\eta = A - \sqrt{A^2 + 1}, \quad B_{\bar{1}} = \bar{A} + \sqrt{\bar{A}^2 + 1}, \quad B_{\bar{1}}^\eta = \bar{A} - \sqrt{\bar{A}^2 + 1}$$

and:

$$X_1(t) = X_1(0)e^{i\sqrt{|\Delta|\sqrt{A^2+1}}t}, \quad X_{\bar{1}}(t) = X_{\bar{1}}(0)e^{i\sqrt{|\Delta|\sqrt{\bar{A}^2+1}}t}$$

The reality condition reads:

$$\overline{X_1(0)}X_{\bar{1}}(0) = -(\overline{B_1})^6 \quad (100)$$

We can express the quantity $\bar{b}b$:

$$\bar{b}b = \frac{|\Delta|}{4} \frac{1}{\Lambda_1\Lambda_2\bar{\Lambda}_1\bar{\Lambda}_2}$$

The spins can be reconstructed through the formula $s_j^z = \frac{P_{n+1}(\epsilon_j)}{\prod_{k \neq j} (\epsilon_j - \epsilon_k)}$. For this we need the polynomial $P_{n+1}(\lambda)$. Adding eqs.(74,75) and using eq.(76) and eq.(72), we get:

$$\Lambda^3 P_3(\Lambda) = 2 \left(\frac{\sqrt{|\Delta|}}{4} \right)^3 \frac{\Lambda^3}{\Lambda_1\Lambda_2\bar{\Lambda}_1\bar{\Lambda}_2} [\Lambda^3 \bar{\mathcal{P}}_+(\Lambda^\eta) \mathcal{P}_+(\Lambda^\eta) + (\Lambda^\eta)^3 \bar{\mathcal{P}}_+(\Lambda) \mathcal{P}_+(\Lambda)]$$

hence:

$$P_3(\Lambda) = 2 \left(\frac{\sqrt{|\Delta|}}{4} \right)^3 \frac{1}{P\bar{P}} \left[P\bar{P}(\Lambda - \Lambda^{-1})^3 + (\bar{P}S + P\bar{S})(\Lambda - \Lambda^{-1})^2 \right. \\ \left. + (S\bar{S} + 3P\bar{P} + P + \bar{P} - 1)(\Lambda - \Lambda^{-1}) + 2(\bar{P}S + P\bar{S} + S + \bar{S}) \right]$$

where:

$$S = \Lambda_1 + \Lambda_2, \quad P = \Lambda_1\Lambda_2, \quad \bar{S} = \bar{\Lambda}_1 + \bar{\Lambda}_2, \quad \bar{P} = \bar{\Lambda}_1\bar{\Lambda}_2$$

From eq.(97), we see that this is polynomial of degree 3 in λ , as it should be.

One can obtain the reality condition expressed directly on (Λ_1, Λ_2) . Eqs.(98,99) are a linear system for the symmetric functions S, P . One can eliminate X and \bar{X} between these equations and their complex conjugate, taking into account eq.(100). The result can be written in the form:

$$\frac{S}{P} + \frac{\bar{S}}{\bar{P}} = -2(A + \bar{A}), \quad \left(1 + \frac{1}{P}\right) \left(1 + \frac{1}{\bar{P}}\right) + \frac{S}{P} \frac{\bar{S}}{\bar{P}} = 4A\bar{A} \quad (101)$$

An example of the motion of the variables Λ_1, Λ_2 is shown in Fig.[7,8], and the associated motions of s_1^z, s_2^z and $\bar{b}b$ are shown in Figs.(9,10). We recover the soliton-like behavior of the large motion already discussed for the rank zero case. One difference is that now, the spins are no longer along the z axis as times goes to $\pm\infty$. But we also see that the pulse in the oscillator energy $\bar{b}b(t)$ develops a non-trivial time dependence, with oscillations superimposed to a typical solitonic envelope. This reflects an important qualitative difference between the rank zero and the rank one case. In the former case, the pre-image is just a two-dimensional pinched torus, whose small cycle corresponds to the global $U(1)$ action generated by H_3 . This cycle is not seen in the reduced model, for which the large motion connecting the unstable manifold to the stable one is one-dimensional. But for a point on a line of rank one, the pre-image is the product of a circle by a two-dimensional pinched torus. As a result, the winding motion around the small cycle of this torus becomes observable for the reduced model, as manifested by Figs.(9,10).

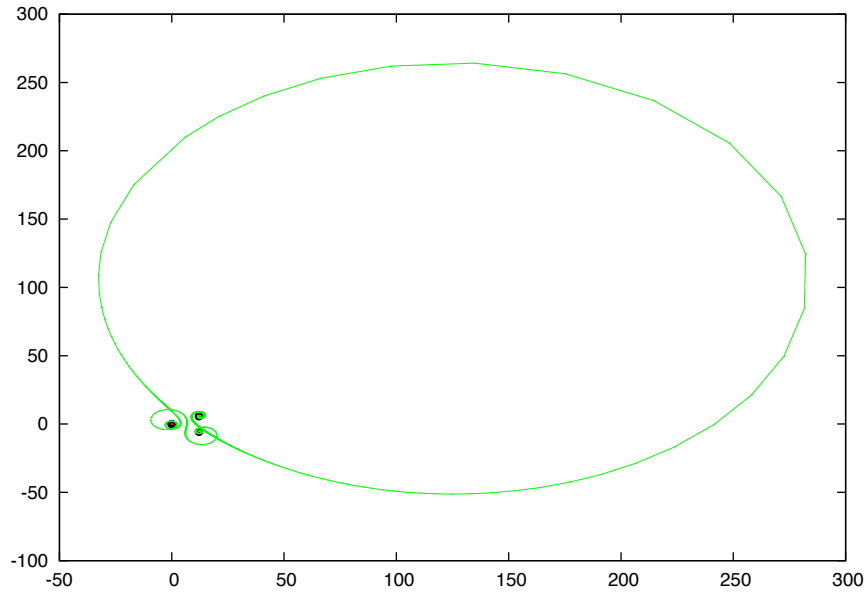


Figure 7: Motion of the point Λ_1 of the divisor. The second point Λ_2 is hidden into the black dot. ($\epsilon_1 = -1.2, \epsilon_2 = -1.735$).

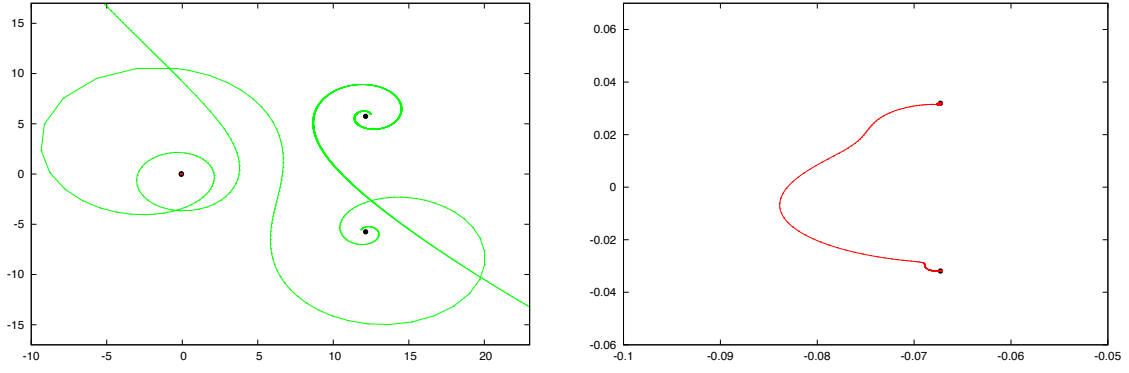


Figure 8: A zoom of the motion of the divisor Λ_1, Λ_2 . ($\epsilon_1 = -1.2, \epsilon_2 = -1.735$).

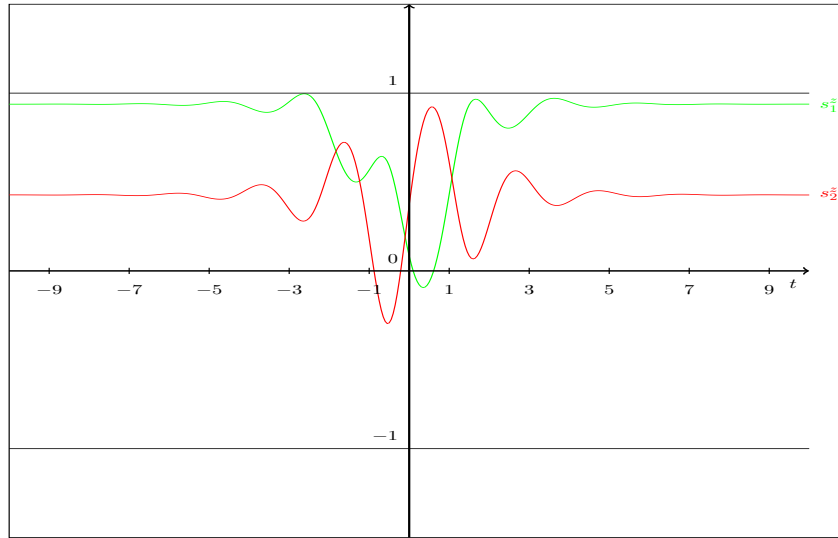


Figure 9: The components s_1^z and s_2^z of the spins. ($\epsilon_1 = -1.2, \epsilon_2 = -1.735$).

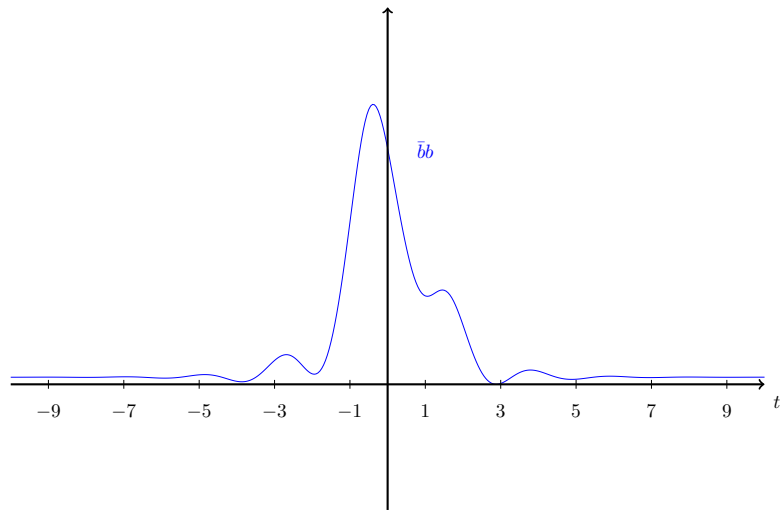


Figure 10: The quantity $\bar{b}b$. ($\epsilon_1 = -1.2, \epsilon_2 = -1.735$).

7 The three spin model.

7.1 Critical stratum of dimension 4

Let us examine in some detail the example of three spins, for which we focus on the case of fully degenerate spectral curves associated to the critical points:

$$b = \bar{b} = 0, \quad s_j^\pm = 0, \quad s_j^z = e_j s, \quad e_j = \pm 1$$

Therefore, the spectral polynomial can be written as:

$$Q_8(\lambda) = 4 \prod_{l=1}^4 (\lambda - E_l)^2$$

According to the general analysis presented in section 4, the different strata in the associated degenerate torus are obtained when $n_0 = 0$ and $n_0 = 2$. Consider first the case $n_0 = 0$, (or in the general case $n_0 = n - 3$). We have:

$$\begin{aligned} \deg \mathcal{P}_+ &= \deg \mathcal{S}_+ = 1 \\ \deg \mathcal{P}_- &= \deg \mathcal{S}_- = 2 \end{aligned}$$

We set:

$$\mathcal{P}_-(\lambda) = \lambda^2 - \sigma_1 \lambda + \sigma_2, \quad \mathcal{P}_+(\lambda) = \lambda - \lambda_0$$

Equations (55) become:

$$\frac{\sigma_2}{b} - E_l \frac{\sigma_1}{b} + E_l^2 \frac{1}{b} + X_l \lambda_0 = E_l X_l, \quad l = 1 \cdots 4.$$

or, in matrix form:

$$\begin{pmatrix} 1 & E_1 & E_1^2 & X_1 \\ 1 & E_2 & E_2^2 & X_2 \\ 1 & E_3 & E_3^2 & X_3 \\ 1 & E_4 & E_4^2 & X_4 \end{pmatrix} \begin{pmatrix} \sigma_2/\bar{b} \\ -\sigma_1/\bar{b} \\ 1/\bar{b} \\ \lambda_0 \end{pmatrix} = \begin{pmatrix} E_1 X_1 \\ E_2 X_2 \\ E_3 X_3 \\ E_4 X_4 \end{pmatrix}$$

We introduce the matrices:

$$\begin{aligned} M_0 &= \begin{pmatrix} 1 & E_1 & E_1^2 & X_1 \\ 1 & E_2 & E_2^2 & X_2 \\ 1 & E_3 & E_3^2 & X_3 \\ 1 & E_4 & E_4^2 & X_4 \end{pmatrix}, \quad M_1 = \begin{pmatrix} 1 & E_1 & E_1^2 & E_1 X_1 \\ 1 & E_2 & E_2^2 & E_2 X_2 \\ 1 & E_3 & E_3^2 & E_3 X_3 \\ 1 & E_4 & E_4^2 & E_4 X_4 \end{pmatrix} \\ M_2 &= \begin{pmatrix} E_1 & E_1^2 & X_1 & E_1 X_1 \\ E_2 & E_2^2 & X_2 & E_2 X_2 \\ E_3 & E_3^2 & X_3 & E_3 X_3 \\ E_4 & E_4^2 & X_4 & E_4 X_4 \end{pmatrix}, \quad M_3 = \begin{pmatrix} 1 & E_1^2 & X_1 & E_1 X_1 \\ 1 & E_2^2 & X_2 & E_2 X_2 \\ 1 & E_3^2 & X_3 & E_3 X_3 \\ 1 & E_4^2 & X_4 & E_4 X_4 \end{pmatrix}, \quad M_4 = \begin{pmatrix} 1 & E_1 & X_1 & E_1 X_1 \\ 1 & E_2 & X_2 & E_2 X_2 \\ 1 & E_3 & X_3 & E_3 X_3 \\ 1 & E_4 & X_4 & E_4 X_4 \end{pmatrix} \end{aligned}$$

Denoting $D_i = \det M_i$ we have:

$$\lambda_0 = \frac{D_1}{D_0}, \quad \sigma_2 = \frac{D_2}{D_4}, \quad \sigma_1 = \frac{D_3}{D_4}, \quad \bar{b} = -\frac{D_0}{D_4} \quad (102)$$

Moreover, eq.(63) becomes:

$$\bar{b}b = \frac{4}{\mathcal{P}_-(\lambda_0)} \left(-\frac{Q(\lambda_1^-) - Q(\lambda_2^-)}{\lambda_1^- - \lambda_2^-} \lambda_0 + \frac{\lambda_2^- Q(\lambda_1^-) - \lambda_1^- Q(\lambda_2^-)}{\lambda_1^- - \lambda_2^-} \right)$$

where we have introduced the polynomial $Q(\lambda)$ (not to be confused with $Q_8(\lambda)$) defined by:

$$Q(\lambda) = \prod_{l=1}^4 (\lambda - E_l)$$

The right hand side in the expression of $\bar{b}b$ is a function of σ_1 and σ_2 since λ_1^- and λ_2^- are the roots of $\mathcal{P}_-(\lambda)$.

In Fig.[11] we show an example of parameters e_j, ϵ_j such that the classical Bethe equation has four complex solutions. Note that if we choose for our critical point the ground-state of the diagonal part of the Hamiltonian $\sum_j 2\epsilon_j s_j^z$, we have $e_j \epsilon_j$ negative for all j , and a simple graphical construction shows that the Bethe equations have at most a single pair of complex conjugate roots. In this case, according to our general discussion, $n_0 = n - 1$ and the preimage is composed of a two dimensional pinched torus, independently of the value of n . In the example of Fig.[11], $(e_1, e_2, e_3) = (1, -1, 1)$ and $(\epsilon_1, \epsilon_2, \epsilon_3) = (-3, -2.7, 0.5)$ so that only $e_1 \epsilon_1$ is negative, and the critical point is a doubly excited state of $\sum_j 2\epsilon_j s_j^z$.

From the general form of the time evolution (55), we see that:

$$\bar{X}_l(t) = \frac{\bar{X}_l(0)}{X_{\bar{l}}(0)} X_{\bar{l}}(-t)$$

and the reality conditions eq. (69) imply then that:

$$\bar{X}_l(t) = -4\bar{X}_l(0)^2 X_{\bar{l}}(-t)$$

As a result, if $X_i^2(0) = 1/4$ then we have $\bar{b}b(-t) = \bar{b}b(t)$ so that $\bar{b}b$ has an extremum at $t = 0$. Only the relative signs of $X_i(0)$ matters. In Fig.[12] we draw the function $\bar{b}b(t)$ when $X_1(0) = X_2(0) = 1/2$. The maximum is at $\bar{b}b(0) = |E_1 + E_2 - \bar{E}_1 - \bar{E}_2|^2$. The time evolution of $\bar{b}b(t)$ shows a rather rich internal structure on top of an overall solitonic shape. Note that this trajectory lies on a stratum of dimension 4, which can be described, at least in the vicinity of the unstable critical point $(e_1, e_2, e_3) = (1, -1, 1)$ where the system is equivalent to its quadratic normal form, as a product of two pinched torii of dimension 2. The complexity of the motion is illustrated in Fig.[13] which shows the trajectory $\lambda_0(t)$ in the case $X_1(0) = X_2(0) = 1/2$. We see that it runs from one of the roots E_i to its complex conjugate. Because the dimension of this stratum is larger than two, it is quite easy to change the shape of these solitonic pulses. An other example is shown in Fig.[14] when $X_1(0) = -X_2(0) = 1/2$. The extremum at $\bar{b}b(0) = |E_1 - E_2 - \bar{E}_1 + \bar{E}_2|^2$ is now a local minimum.

7.2 Critical stratum of dimension N

These observations can be extended for a system with an arbitrary number of spins. Let us consider a stratum of dimension N containing a critical point, where N is the number of roots which don't correspond to any frozen separated variable λ_i . We have $N = n + 1 - n_0 = n_- + n_+ + 1$ and N is even because $n_- - n_+ = 1$. In general, \bar{b} can be written as the ratio of two determinants of size N , that is $\bar{b} = (-1)^{n_+} D_0 / D_{n+1}$ where:

$$D_0 = 1 \wedge E \wedge E^2 \cdots \wedge E^{n_-} \wedge X \wedge XE \cdots \wedge XE^{(n_+ - 1)} \quad (103)$$

$$D_{n+1} = 1 \wedge E \wedge E^2 \cdots \wedge E^{(n_- - 1)} \wedge X \wedge XE \cdots \wedge XE^{n_+} \quad (104)$$

Notice that the degree in energy of these determinants are:

$$d_0 = \frac{n_-(n_- + 1)}{2} + \frac{n_+(n_+ - 1)}{2}$$

$$d_{n+1} = \frac{n_-(n_- - 1)}{2} + \frac{n_+(n_+ + 1)}{2}$$

so that

$$d_0 - d_{n+1} = n_- - n_+ = 1$$

At the symmetric point $X_i(t=0) = X_i(0) = 1/2$, we have:

$$D_{n+1} = \prod_{i < j} (E_i - E_j)(\bar{E}_i - \bar{E}_j)$$

$$D_0 = D_{n+1} \sum_i (E_i - \bar{E}_i) = 2i D_{n+1} \sum_i \text{Im} E_i$$

All $\text{Im} E_i$ are positive, so assuming that they are of order one:

$$\bar{b}b(0) \geq N^2 |\min \text{Im} E_i|^2$$

and we recover the super radiance phenomenon of Dicke.

7.3 Critical stratum of minimal dimension

We consider now the case with $n_0 = 2$ frozen roots. This gives a smaller stratum of dimension two. In the general case we would take $n_0 = n - 1$. We have:

$$\deg \mathcal{P}_+ = \deg \mathcal{S}_+ = 0$$

$$\deg \mathcal{P}_- = \deg \mathcal{S}_- = 1$$

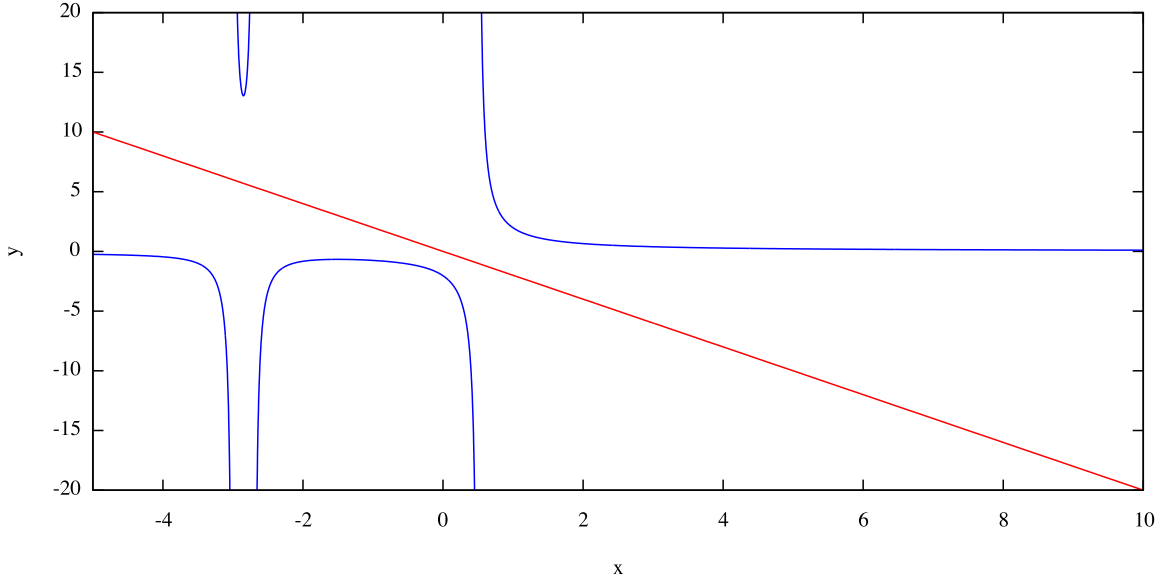


Figure 11: The 3 spins model. Determination of the parameters ϵ_i such that the classical Bethe equation has 4 complex roots. The blue curve is $y = se_1/(x - \epsilon_1) + se_2/(x - \epsilon_2) + se_3/(x - \epsilon_3)$, the red curve is the straight line $y = -2x$. $(e_1, e_2, e_3) = (1, -1, 1)$, $(\epsilon_1, \epsilon_2, \epsilon_3) = (-3, -2.7, 0.5)$.

We choose to freeze (λ_2, λ_3) at (E_2, \bar{E}_2) . So λ_1 is the only separated variable which is not frozen. We can write:

$$\mathcal{P}_-(\lambda) = (\lambda - \lambda_1), \quad \mathcal{P}_+(\lambda) = 1, \quad \mathcal{P}_0(\lambda) = (\lambda - E_2)(\lambda - \bar{E}_2)$$

The conditions eq.(55) give

$$\mathcal{P}_-(E_1) = \bar{b}X_1, \quad \mathcal{P}_-(\bar{E}_1) = \bar{b}X_{\bar{1}} \quad (105)$$

which are solved by:

$$\lambda_1 = \frac{\bar{E}_1 X_1 - E_1 X_{\bar{1}}}{X_1 - X_{\bar{1}}}, \quad \bar{b} = \frac{E_1 - \bar{E}_1}{X_1 - X_{\bar{1}}} \quad (106)$$

where:

$$\overline{X_1(0)} X_{\bar{1}}(0) = -\frac{1}{4}$$

The last equality yields the familiar compatibility relation:

$$\lambda_1 + \bar{\lambda}_1 = E_1 + \bar{E}_1 \quad (107)$$

Since the unfrozen pair can be (E_i, \bar{E}_i) , $i = 1 \cdots n$, we have n such solutions. We show an example of the small strata in Fig.[15]. We recover a simple solitonic pulse, in agreement with the general

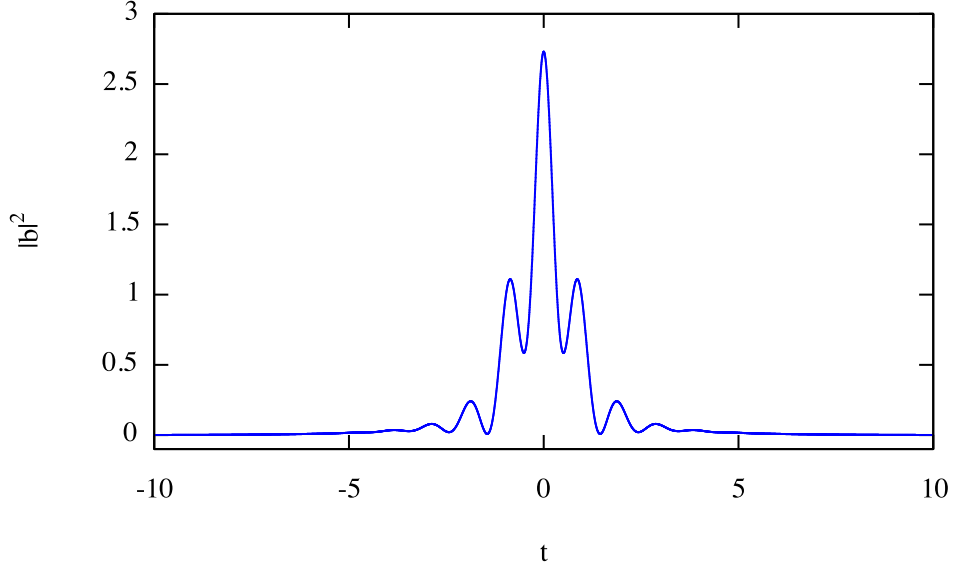


Figure 12: The 3 spins model. $\bar{b}b(t)$ as function of time. $X_1(0) = X_2(0) = 1/2$

idea, discussed in subsection 2.3 that in this case, the system dynamics can be mapped into the one of an effective model with a single spin.

7.4 Relation with Normal coordinates.

A natural question is to compare the exact solution Eq.(102) to the normal modes expansion Eq.(116). Normal modes are defined near a critical point which is precisely the pinch of the torus. So, we have to examine the exact solution near the pinch, that is to say when time $t \rightarrow \pm\infty$.

As we describe in section 9, normal coordinates are of the form $B_i \equiv B(E_i)$, $C_i \equiv C(E_i)$, where E_i are the $n + 1$ double roots of the spectral polynomial. There, we show that:

$$C_i(t) = C_i(0)e^{i(\omega+2E_i)t}$$

This implies that $C_i(t)$ remains proportional to $1/X_i(t)$, and we can choose the initial condition so that

$$C_i(t) = \frac{1}{X_i(t)}$$

hence, using Eq.(116):

$$\bar{b}(t) = \sum_i \frac{1}{a'_i} \frac{1}{X_i(t)}$$

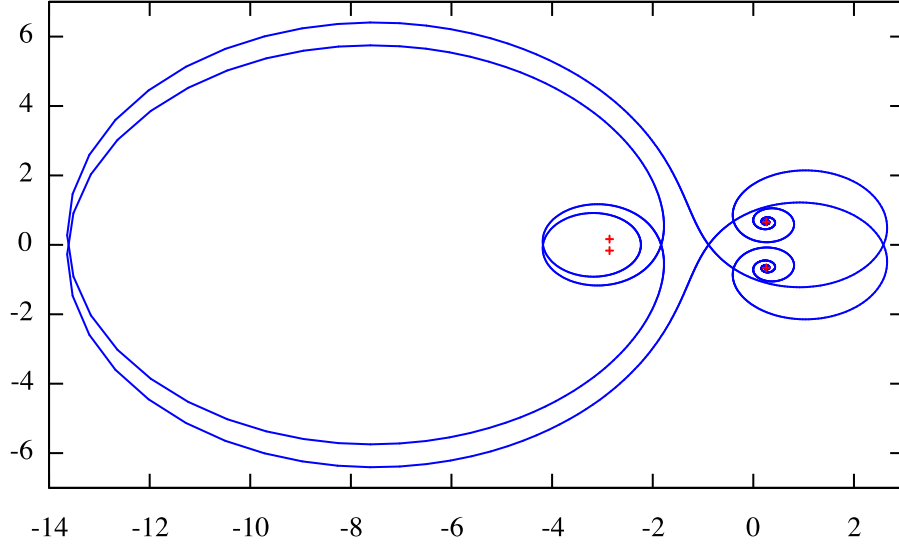


Figure 13: The 3 spins model. The trajectory of λ_0 .

When $t \rightarrow \infty$, $X_i(t) \rightarrow 0$ or ∞ . Since $\bar{b}b$ remains bounded, terms with $X_i(t) \rightarrow 0$ cannot appear when we take the limit of an exact solution. So, when $t \rightarrow -\infty$ only terms with $\text{Im } E_i < 0$ contribute, and when $t \rightarrow +\infty$ only terms with $\text{Im } E_i > 0$ contribute. By definition, we call E_i those classical Bethe roots with $\text{Im } E_i > 0$. Then $E_{\bar{i}} = \bar{E}_i$ has $\text{Im } E_{\bar{i}} < 0$.

The simplest case is given by the stratum of minimal dimension Eq.(106):

$$\bar{b}_{\min}(t) = \frac{E_i - E_{\bar{i}}}{X_i(t) - X_{\bar{i}}(t)}$$

Then

$$\bar{b}_{\min}(t)|_{t \rightarrow -\infty} = -\frac{E_i - E_{\bar{i}}}{X_{\bar{i}}(t)}, \quad \bar{b}_{\min}(t)|_{t \rightarrow +\infty} = \frac{E_i - E_{\bar{i}}}{X_i(t)}$$

So, we find the remarkable result that $\bar{b}_{\min}(t)$ is an exact solution which interpolates between the single normal modes C_i and $C_{\bar{i}}$ at $t = \pm\infty$. In terms of separated variables, this corresponds to $n-1$ variables λ_i frozen on $n-1$ of the E_i , and the last λ_i moving between E_i and $E_{\bar{i}}$. As $t \rightarrow \pm\infty$, $\lambda_i \rightarrow E_i, E_{\bar{i}}$ and the normal modes correspond to all λ_i frozen.

More generally, when we consider the limit at $t \rightarrow -\infty$ in Eqs.(103,104), we should keep the

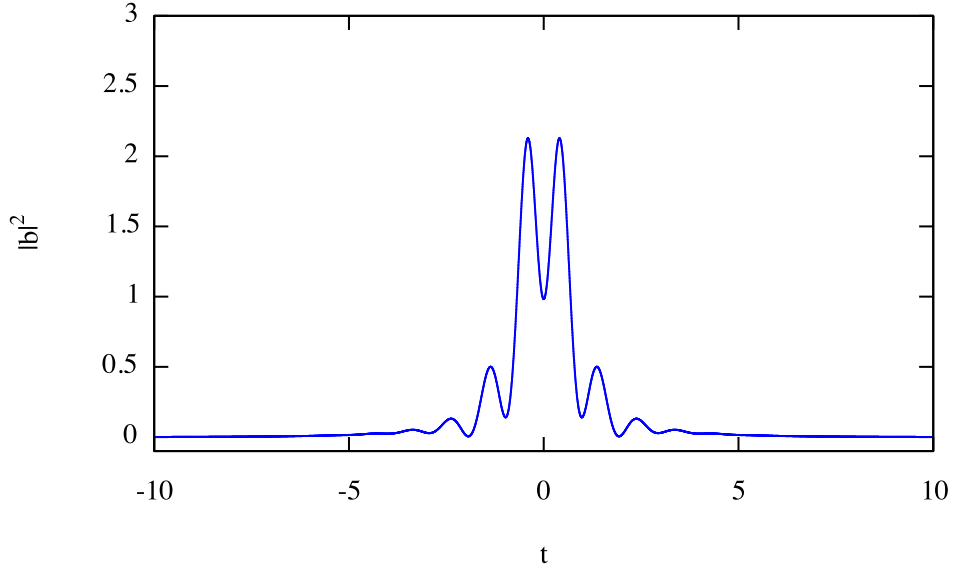


Figure 14: The 3 spins model. $\bar{b}b(t)$ as function of time. $X_1(0) = 1/2, X_2(0) = -1/2$

dominant terms, which amounts to replacing (assuming for simplicity that all roots are complex):

$$X \rightarrow \begin{pmatrix} 0 \\ \vdots \\ 0 \\ X_{\bar{1}} \\ \vdots \\ X_{\overline{n+1}} \end{pmatrix}$$

Then:

$$\bar{b}(t)|_{t \rightarrow -\infty} = \sum_{\bar{i}} \frac{\prod_j (E_{\bar{i}} - E_j)}{\prod_{\bar{j} \neq \bar{i}} (E_{\bar{i}} - E_{\bar{j}})} \frac{1}{X_{\bar{i}}(t)}, \quad \bar{b}(t)|_{t \rightarrow +\infty} = \sum_i \frac{\prod_{\bar{j}} (E_i - E_{\bar{j}})}{\prod_{j \neq i} (E_i - E_j)} \frac{1}{X_i(t)}$$

Hence, the solution appears as a superposition of normal modes at $t \rightarrow -\infty$ and the above formulae determine the asymptotic behavior at $t = +\infty$. Of course, in between, the solution is a non linear superposition of normal modes which is completely beyond the scope of the quadratic normal form, because it describes a motion that starts from the unstable manifold on the critical torus and eventually returns to the stable manifold, after a big motion on the torus. The quadratic normal form is on the other hand very useful to describe trajectories in the vicinity of the critical point

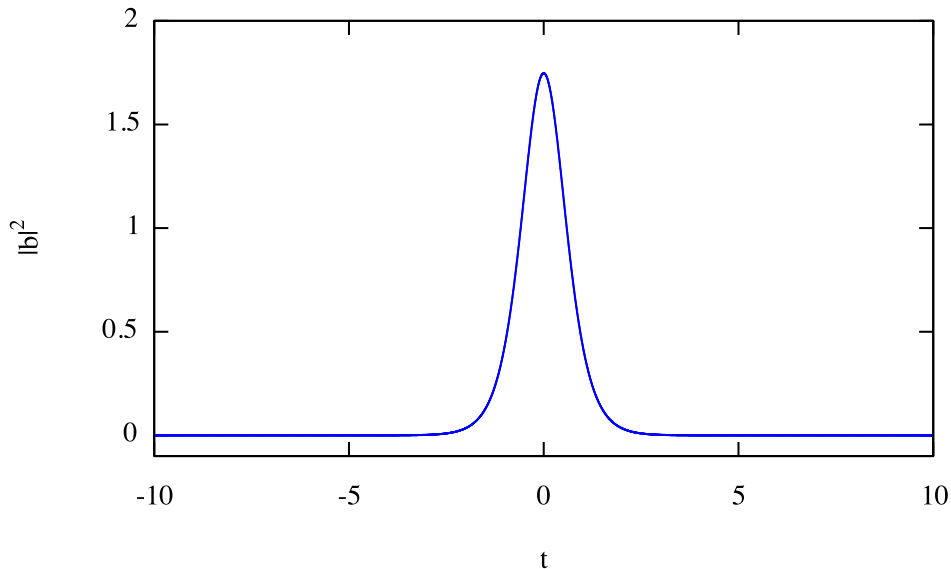


Figure 15: The 3 spins model. The curve $\bar{b}b(t)$ on the small stratum. $X_2(0) = 0.5$.

but on a different pre-image of the moment map, which begin close to the stable manifold, and get kicked towards the unstable one. As for the single spin case, a generic trajectory on a torus close to the critical one will consist in two parts, one well described by the quadratic normal form, and the other well approximated by the generalized solitonic pulses constructed in this section.

The various strata of the real slice are characterized by the number of modes appearing in the expansion of the solution at say $t = -\infty$. In principle this could be controlled by sending some initial conditions $X_{\bar{i}}(0)$ to ∞ . But because of the reality conditions, this is a rather singular limit, and that is why an independent description of each stratum is necessary.

8 Conclusion

In this work, we have analyzed in detail singular torii in the classical integrable Dicke-Jaynes-Cummings-Gaudin model which describes a system of n inequivalent spins coupled to a single harmonic oscillator. These singular torii correspond to critical values of the moment map constructed from the conserved quantities under the Hamiltonian dynamics. The level sets associated to such critical values appear to have a natural stratification, the dimension of each stratum being equal to the rank of the differential of the moment map. Although the complexified model is the natural stage for the algebro-geometric method used to solve Hamilton's equations of motion,

from a physical perspective, it is crucial to look at these level sets on the *real slice*, whose precise identification has been one of the main goals of this work.

The dimension of a stratum on a singular level set is given by $n + 1 - n_0$ where n_0 is the number of separated variables [15] which are frozen on some double roots of the associated spectral polynomial $Q_{2n+2}(\lambda)$. The values of n_0 vary among the integers ranging between the number of real double roots of $Q_{2n+2}(\lambda)$ and the total number of double roots of this polynomial, given the fact that frozen roots occur in complex conjugate pairs. The fact that the possible dimensions of strata belonging to a given level set vary by multiples of 2 has a simple interpretation. We know that singularities in the Dicke-Jaynes-Cummings-Gaudin model have a quadratic normal form which can be either of elliptic or focus-focus type [11]. The quadratic normal form gives a picture of a stratum on a level set that is, in the vicinity of a critical point, the product of an m -dimensional torus and p two-dimensional pinched torii. This gives a stratum of dimension $m + 2p$ where p ranges from zero to the number of distinct focus-focus singularities appearing in the quadratic normal form, which is equal to the number of complex conjugate pairs of double roots of the spectral polynomial. The total number of double roots of this polynomial is then equal to $n + 1 - m$.

We gave a complete parametrization of the real slice for generic torii only in the simplest case of a single spin. Fortunately, these real slices can be explicitly constructed for arbitrary n on level sets of the moment map containing very *small* strata, of minimal dimension $m = 0$ (unstable critical points) or $m = 1$. The former case corresponds to isolated critical values and the latter case to curves in the target space of the moment map. For these two situations, we have shown that it is possible to identify the physical strata of arbitrary dimensions in the corresponding level sets. In the case $m = 0$, the spectral polynomial has $n + 1$ double roots, and we recover the *normal solitons* constructed by Yuzbashyan [12]. When $m = 1$, $Q_{2n+2}(\lambda)$ has only n double roots, but it defines a rational spectral curve, which allowed us to obtain the general form of the *anomalous solitons* discussed by Yuzbashyan [12]. We emphasize that these solitons can involve an arbitrary number of degrees of freedom, equal to the number of independent focus-focus singularities present in the quadratic normal form in the vicinity of the stratum of minimal dimension.

This work raises several open questions. On the theoretical side, the most difficult seems to be to construct the real slice for level sets which contain a stratum of minimal dimension $m \geq 2$. For $m = 2$, the spectral curve can be uniformized by a non-singular curve of genus one, so we may hope, using Weierstrass functions, to find an explicit solution generalizing those we found for $m = 0$ and $m = 1$.

Another question is the quantum counterpart of these multi-mode solitons. If the quantum system is prepared in the separable state where each spin j is in the eigenstate of s_j^z with the eigenvalue se_j , $e_j = \pm 1$, and the oscillator in the ground-state of b^+b , how will such state evolve quantum-mechanically? The problem is to decompose this initial state in the eigenvector basis of the quantum Hamiltonian. Some previous works have addressed this question in the case of a classical pinched torus of dimension 2 [17, 18, 19], where the problem can be mapped into the evolution of a quantum wave packet for a single degree of freedom, prepared initially at the top of an unstable potential barrier. A complicated aperiodic sequence of pulses is obtained, each of them

being close to the classical monomode pulse of the $n = 1$ model. We suspect that the qualitative difference between classical and quantum evolutions will be more pronounced in the case of a critical level set of dimension larger than 2. Intuitively, we expect that quantum fluctuations perform some averaging over the configuration space of the multimode pulses whose result may be quite different from any classical pulse chosen in this ensemble. The theoretical challenge here is to extend the previous semi-classical analysis [17, 18, 19] to a system with several degrees of freedom.

Finally, we hope that some of the aspects of the integrable dynamics discussed here will be evidenced experimentally. As already mentioned in the Introduction, one possibility is to consider cold gases of fermionic atoms in which an attractive interaction is switched on suddenly by sweeping the external magnetic field through a Feshbach resonance [8, 9]. The problem with this system is that it is most conveniently prepared in the ground-state of a weakly interacting Fermi liquid. After crossing the Feshbach resonance, this state becomes an unstable equilibrium point with only one focus-focus singularity in its normal form. So this gives rise only to the elementary single mode soliton. As shown in section 7, we need to start with an excited eigenstate of the diagonal part of the Hamiltonian to have a chance to observe multi-mode solitons. In this respect, another class of systems looks promising. Recently, several experimental groups have succeeded to couple a single quantum oscillator to a collection of electronic spins [20, 21, 22, 23]. These experiments are in a regime where the spin ensemble behaves nearly as a macroscopic oscillator, so most-likely in a regime close to the ground-state of the coupled system. But it seems that such systems allow various manipulations [20, 25], potentially useful for the long time storage of quantum information. We hope that they will provide a route to access also some of the interesting physics controlled by unstable critical points, which has been the main focus of the present work.

9 Appendix: Normal form around critical points

Critical points are equilibrium points for all the Hamiltonians H_j , $j = 1, \dots, n+1$. At such points the derivatives with respect of all coordinates on phase space vanish. We have 2^n critical points located at:

$$b = \bar{b} = 0, \quad s_j^\pm = 0, \quad s_j^z = e_j s, \quad e_j = \pm 1 \quad (108)$$

When we expand around a configuration given by eq.(108), all the quantities $(b, \bar{b}, s_j^+, s_j^-)$ are first order, but s_j^z is second order because $s_j^z = s e_j - \frac{e_j}{2s} s_j^+ s_j^- + \dots$, $e_j = \pm 1$. It is then simple to see that all first order terms in the expansions of the Hamiltonians H_j vanish. In particular, we can replace the dynamical generating function $A(\lambda)$ defined by eq. (10) by its non-dynamical approximation:

$$a(\lambda) = 2\lambda + \sum_j \frac{s e_j}{\lambda - \epsilon_j}$$

We can expand the Hamiltonians H_j around the equilibrium points eq.(108) and write them in normal form. Normal modes are obtained as follows. Consider the equation:

$$a(E) = 2E + \sum_j \frac{se_j}{E - \epsilon_j} = 0, \quad \text{“Classical Bethe Equation”} \quad (109)$$

This is an equation of degree $n + 1$ for E . Calling E_i its solutions, we construct in this way $n + 1$ variables $C_i \equiv C(E_i)$ and conjugated variables $B_i \equiv B(E_i)$. We have:

$$\{C_i, C_j\} = 0, \quad \{B_i, B_j\} = 0 \quad (110)$$

and

$$\{B_i, C_j\} = 2ia'_i \delta_{ij} \quad (111)$$

where a'_i stands for $a'(E_i)$. Up to normalisation, these are canonical coordinates. It is simple to express the quadratic Hamiltonians in these coordinates:

$$\frac{1}{2} \text{Tr} L^2(\lambda) = a^2(\lambda) + \sum_j \frac{a(\lambda)}{a'_j(\lambda - E_j)} B_j C_j \quad (112)$$

This has the correct analytical properties in λ and in particular, there is no pole at $\lambda = E_j$ because $a(E_j) = 0$. Expanding around $\lambda = \infty$ we get:

$$H_{n+1} = s \sum_k e_k + \sum_i \frac{1}{2a'_i} B_i C_i$$

and computing the residue at $\lambda = \epsilon_j$, we find:

$$H_j = se_j \left[2\epsilon_j + \sum_k \frac{se_k}{\epsilon_j - \epsilon_k} \right] + \sum_i \frac{1}{2a'_i} \frac{se_j}{\epsilon_j - E_i} B_i C_i$$

The physical Hamiltonian is then:

$$H = H_{cp} + \sum_i \frac{\omega + 2E_i}{2a'_i} B_i C_i \quad (113)$$

where H_{cp} is the total energy at the critical point. This expression, together with Poisson brackets (110) and (111), shows that the eigenfrequencies for the linearized equations of motion under the Hamiltonian H are $\pm(\omega + 2E_i)$.

We can invert these formulae: divide eq.(112) by $\lambda - E_j$ and take the residue at $\lambda = E_j$. Since $a(E_j) = 0$ we get:

$$\frac{1}{2} \text{Tr} L^2(E_j) = B_j C_j$$

or explicitly:

$$B_j C_j = 4E_j^2 + 4H_{n+1} + \sum_{k=1}^n \frac{2H_k}{E_j - \epsilon_k} + \sum_{k=1}^n \frac{s^2}{(E_j - \epsilon_k)^2}$$

Let us express now the first order quantities b, \bar{b}, s_j^+, s_j^- in terms of the normal coordinates B_i, C_i . For this, we can reconstruct the generating functions $B(\lambda)$ and $C(\lambda)$. In fact:

$$B(\lambda) = \frac{N(\lambda)}{\prod_k (\lambda - \epsilon_k)}$$

where $N(\lambda)$ is a polynomial of degree n and we know its values at the $n + 1$ classical Bethe roots:

$$N(E_i) = B_i \prod_k (E_i - \epsilon_k)$$

Hence we can reconstruct it by Lagrange interpolation formula:

$$N(\lambda) = \sum_i B_i \frac{\prod_k (E_i - \epsilon_k) \prod_{j \neq i} (\lambda - E_j)}{\prod_{j \neq i} (E_i - E_j)}$$

Now:

$$a'_i = 2 \frac{\prod_{j \neq i} (E_i - E_j)}{\prod_k (E_i - \epsilon_k)}$$

so we can write:

$$B(\lambda) = 2 \sum_i B_i \frac{1}{a'_i} \frac{\prod_{k \neq i} (\lambda - E_k)}{\prod_j (\lambda - \epsilon_j)} \quad (114)$$

and similarly:

$$C(\lambda) = 2 \sum_i C_i \frac{1}{a'_i} \frac{\prod_{k \neq i} (\lambda - E_k)}{\prod_j (\lambda - \epsilon_j)} \quad (115)$$

Computing the leading terms at ∞ we find:

$$b = \sum_i \frac{1}{a'_i} B_i, \quad \bar{b} = \sum_i \frac{1}{a'_i} C_i \quad (116)$$

Computing the residue at $\lambda = \epsilon_j$ we get:

$$s_j^- = 2 \frac{\prod_k (\epsilon_j - E_k)}{\prod_{k \neq j} (\epsilon_j - \epsilon_k)} \sum_i \frac{1}{a'_i (\epsilon_j - E_i)} B_i$$

We can simplify this formula. Using the definition of classical Bethe roots

$$a(\lambda) = 2\lambda + \sum_j \frac{se_j}{\lambda - \epsilon_j} = 2 \frac{\prod_i (\lambda - E_i)}{\prod_k (\lambda - \epsilon_k)}$$

and calculating the residue at $\lambda = \epsilon_j$ we find:

$$se_j = 2 \frac{\prod_k (\epsilon_j - E_k)}{\prod_{k \neq j} (\epsilon_j - \epsilon_k)}$$

hence:

$$s_j^- = se_j \sum_i \frac{1}{a_i'(\epsilon_j - E_i)} B_i, \quad s_j^+ = se_j \sum_i \frac{1}{a_i'(\epsilon_j - E_i)} C_i$$

The reality conditions are easily expressed in this approximation. From $B(\lambda) = C(\lambda^*)^*$, we get:

$$B_i = C_i^*$$

where C_i stands for $C(\bar{E}_i)$. From Eq. (115), it is possible to describe the pattern of separated variables λ_α corresponding to the vicinity of the critical point on the critical torus. Using Eq. (113), we see that this critical torus is defined, within the quadratic approximation, by:

$$B_i C_i = 0$$

for any i . For a real root E_i , the reality condition implies $B_i = C_i^*$ so $B_i = C_i = 0$ and we have one separated variable λ_α frozen at E_i . Let us now consider a complex root E_i . Using the decomposition Eq.(113) of the physical Hamiltonian in normal modes, and Eqs.(110,111) for Poisson brackets, we find:

$$\partial_t C_i = \{H, C_i\} = i(\omega + 2E_i)C_i$$

so that:

$$C_i(t) = C_i(0)e^{i(\omega+2E_i)t}$$

The tangent cone to the critical torus at the critical point is composed of two hyperplanes. The first one corresponds to unstable directions, for which $C_i(t)$ grows as time increases, that is $\Im E_i < 0$. The second one is associated to stable directions, given by $\Im E_i > 0$. Generically, on the unstable hyperplane, the expression (115) for $C(\lambda)$ is dominated at large times by the term such that $\Im E_i < 0$ with largest absolute value. Eq. (115) shows that in this case, all the separated variables are located on the n roots E_j different from E_i . On a codimension one subspace on the unstable hyperplane, the coefficient $C_i(0)$ of this leading eigenvalue vanishes, and the subleading root becomes non-frozen. More generally, $C(\lambda)$ is dominated at large times by the term for which $\text{Im } E_i$ is negative and of maximal absolute value among the i 's such that $C_i(0) \neq 0$.

Similarly, the stable hyperplane exhibits a nested sequence of linear subspaces, each of which corresponds to freezing the separated variables on all the roots E_j excepted one root E_i with positive imaginary part.

References

- [1] R. H. Dicke, *Coherence in spontaneous radiation processes*, Phys. Rev. **93**, 99 (1954).
- [2] J. M. Raimond, M. Brune, and S. Haroche, *Manipulating quantum entanglement with atoms and photons in a cavity*, Rev. Mod. Phys. **73**, 565-582, (2001).
- [3] A. Blais, R.-S. Huang, A. Walraff, S. M. Girvin, and R. J. Schoelkopf, *Cavity quantum electrodynamics for superconducting electrical circuits: An architecture for quantum computation*, Phys. Rev. A **69**, 062320, (2004).
- [4] M. Gaudin, **La Fonction d' Onde de Bethe**. Masson, (1983).
- [5] E. Yuzbashyan, V. Kuznetsov, B. Altshuler, *Integrable dynamics of coupled Fermi-Bose condensates*. Phys. Rev. B **72** (2005), p. 144524.
- [6] E. Jaynes, F. Cummings, Proc. IEEE vol. 51 (1963) p. 89.
- [7] M. Brune, F. Schmidt-Kaler, A. Maali, J. Dreyer, E. Hagley, J. M. Raimond, and S. Haroche, *Quantum Rabi Oscillation: A Direct Test of Field Quantization in a Cavity*, Phys. Rev. Lett. **76**, 1800-1803, (1996).
- [8] R. A. Barankov, and L. S. Levitov, *Atom-Molecule Coexistence and Collective Dynamics Near a Feshbach Resonance of Cold Fermions*, Phys. Rev. Lett. **93**, 130403, (2004)
- [9] R. A. Barankov, L. S. Levitov, and B. Z. Spivak, *Collective Rabi Oscillations and Solitons in a Time-Dependent BCS Pairing Problem*, Phys. Rev. Lett. **93**, 160401, (2004)
- [10] L. H. Eliasson *Normal forms for Hamiltonian systems with Poisson commuting integrals - elliptic case* Comment. Math. Helvetici 65 (1990) pp. 4-35.
- [11] O. Babelon, B. Douçot, *Classical Bethe Ansatz and Normal Forms in the Jaynes-Cummings Model*. arXiv:1106.3274
- [12] E. A. Yuzbashyan, *Normal and anomalous solitons in the theory of dynamical Cooper pairing*, Phys. Rev. B **78**, 184507, (2008).
- [13] B.A. Dubrovin, I.M. Krichever, S.P. Novikov, *Integrable Systems I*. Encyclopedia of Mathematical Sciences, Dynamical systems IV. Springer (1990) p.173–281.
- [14] O. Babelon, D. Bernard, M. Talon, **Introduction to Classical Integrable systems**. Cambridge University Press (2003).
- [15] E. Sklyanin, *Separation of variables in the Gaudin model*. J. Soviet Math., Vol. 47, (1979) pp. 2473-2488.

- [16] M. Audin, *Spinning tops*, Cambridge University Press 1996.
- [17] R. Bonifacio and R. Preparata, *Coherent spontaneous emission*, Phys. Rev. A **2**, 336 (1970).
- [18] O. Babelon, B. Douçot, L. Cantini, *A semiclassical study of the Jaynes-Cummings model.*, J. Stat. Mech. (2009) P07011.
- [19] J. Keeling, *Quantum corrections to the semiclassical collective dynamics in the Tavis-Cummings model*, Phys. Rev. A **79**, 053825, (2009).
- [20] Y. Kubo et al., *Strong Coupling of a Spin Ensemble to a Superconducting Resonator*, Phys. Rev. Lett. **105**, 140502 (2010).
- [21] D. I. Schuster et al., *High-Cooperativity Coupling of Electron-Spin Ensembles to Superconducting Cavities*, Phys. Rev. Lett. **105**, 140501 (2010).
- [22] R. Amsuss et al., *Cavity QED with Magnetically Coupled Collective Spin States*, Phys. Rev. Lett. **107**, 060502, (2011).
- [23] P. Bushev et al., *Ultralow-power spectroscopy of a rare-earth spin ensemble using a superconducting resonator*, Phys. Rev. B **84**, 060501(R) (2011)
- [24] Y. Kubo et al., *Hybrid Quantum Circuit with a Superconducting Qubit Coupled to a Spin Ensemble*, Phys. Rev. Lett. **107**, 220501, (2011).
- [25] Hua Wu et al., *Storage of Multiple Coherent Microwave Excitations in an Electron Spin Ensemble*, Phys. Rev. Lett. **105**, 140503, (2010).
- [26] John Williamson, *On the Algebraic Problem Concerning the Normal Forms of Linear Dynamical Systems*. American Journal of Mathematics, Vol. 58 No. 1 (1936), pp. 141-163.
- [27] V. I. Arnold, *Mathematical Methods of Classical Mechanics*, Springer, New-York, 1997, Appendix 6.
- [28] M. F. Atiyah, *Convexity and commuting Hamiltonians*. Bull. London Math. Soc. 14(1) (1982) pp. 1-15.
- [29] V. Guillemin, S. Sternberg, *Convexity properties of the momentum mapping*. Invent. Math. 67(3) (1982) pp. 491-513.
- [30] San Vũ Ngọc *Moment polytopes for symplectic manifolds with monodromy*. Adv. Math. **208** (2007), pp. 909-934

- [31] H. Duistermaat, *On Global Action-Angle variables*, Comm. Pure Appl. Math. 33 (1980) pp. 687-706.
- [32] Alvaro Pelayo, San Vũ Ngoc. *Hamiltonian dynamics and spectral theory for spin-oscillators*. ArXiv 1005.0439.
- [33] I. Krichever, *“Hessians” of integrals of the Korteweg-De Vries Equation and Perturbations of Finite-Zone Solutions*. Soviet Math. Dokl. Vol. 27 (1983), No. 3, pp. 757-761.
- [34] M. Audin, *Hamiltonian Monodromy via Picard-Lefschetz theory*. Comm. Math. Phys. 229 (2002) pp. 459-489.
- [35] M. Zou, *Monodromy in two degrees of freedom integrable systems*, J. Geom. Phys. **10**, (1992) p. 37.
- [36] N. T. Zung, *A note on focus-focus singularities*, Lett. Math. Phys. **60**, (2002), pp. 87-99.
- [37] N. T. Zung, *Another note on focus-focus singularities*, Diff. Geom. Appl. **7**, (1997), p. 123.
- [38] R. Cushman and J. J. Duistermat, *Non-Hamiltonian monodromy*, J. Diff. Eqs. **172**, (2001) p. 42.
- [39] O. Babelon, M. Talon, *Riemann surfaces, separation of variables and classical and quantum integrability*. Phys. Lett. A. 312 (2003), pp. 71-77.
- [40] P. Griffiths and J. Harris, *Principles of algebraic geometry*, Wiley, New-York (1978), chapter 2.
- [41] O. Babelon, D. Talalaev, *On the Bethe Ansatz for the Jaynes-Cummings-Gaudin model*. J. Stat. Mech. (2007) P06013.